Porous silicon and Si nanoparticles: new photonic and electronic materials

Part 2. Applications

проф. В.А.Скришевський

Porous & nano-Si

Preparation Methods

Properties

Morphology, structure, chemical composition

- -Technology (stressed Si layer, SOI, Sirepitaxy)
- -Hydrogen reservoir
- -Explosive material
- -Support matrix for sensors and thin film solar cell

Optical & Luminescent

- -Chemical & bio-sensors (sensing layer & transducer)
- -Waveguides & fibers
- -Photonic crystals
- -Microcavities and mirrors
- -Solar cells (antireflection & passivation coating, PhL, QD)

Electronics & electrics

- -LED, laser
- -Chemical & bio-sensors (transducer)
- -Functional elements of microelectronics

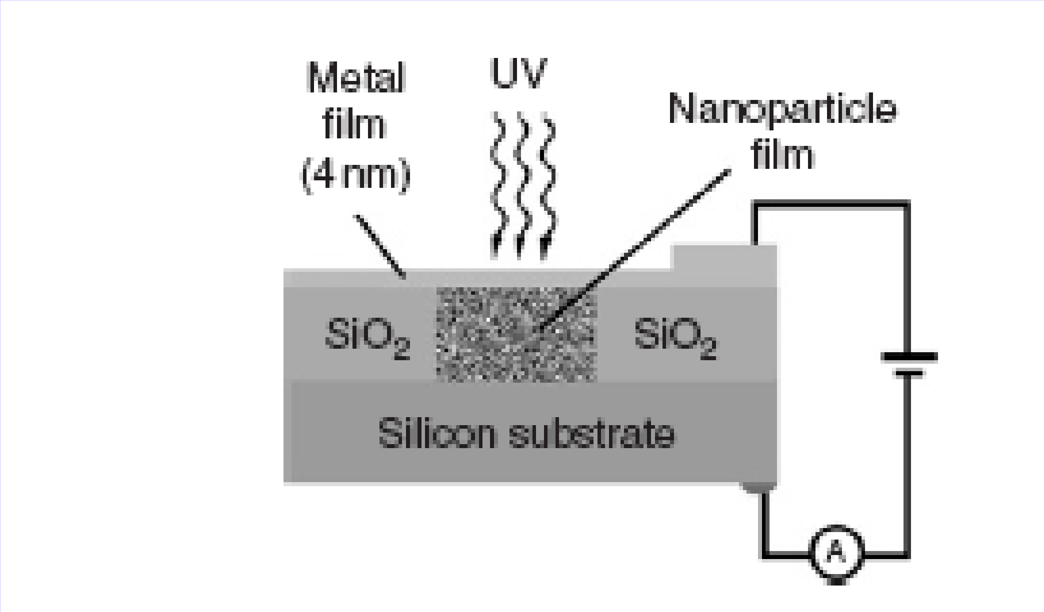

UV photodetector

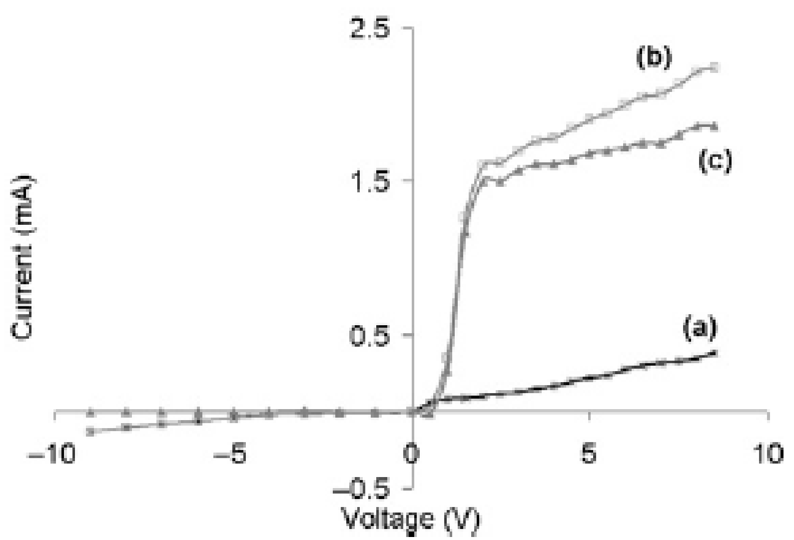

Figure 1.55 *I–V* spectra at room temperature: (a) taken under dark condition, (b) taken under light irradiation. It shows a high visibility regular step structure, for negative tip biasing, and (c) the difference of (b) and (a)

λ=365 nm, 2mV, No sensing in visible region

V.Kumar, Nanosilicon, Elsevier, 2007

Electroluminescence of porous Si (injection-type in Schottky contact)

Requerements:
λ=0.4-0.7 μm (displays), 1.3-1.6 (optical fibers)
Emitting power in mW range
Operating voltage <5 V
Modulation frequency- few kHz (display),
> Few GHz(communications)

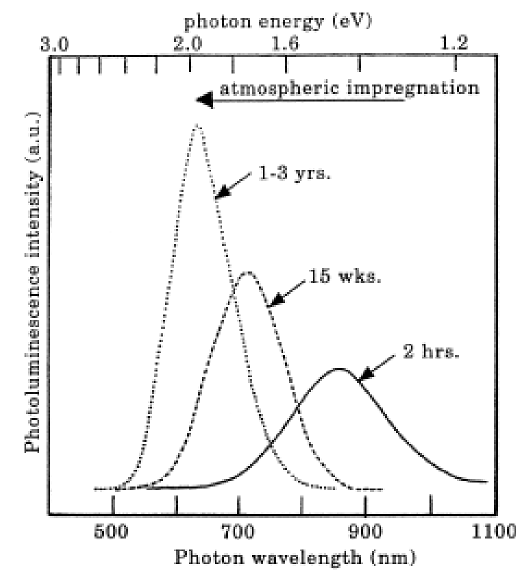

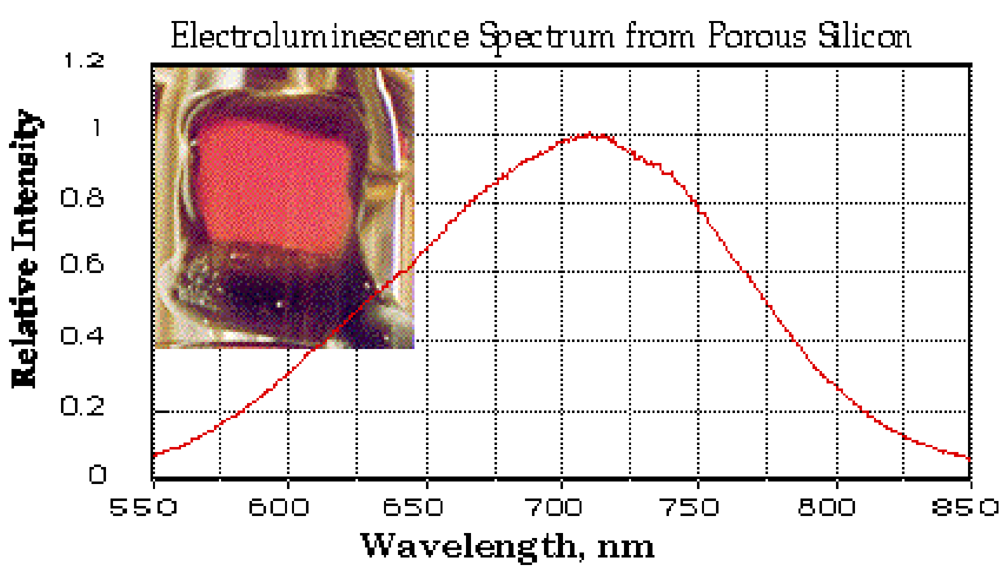

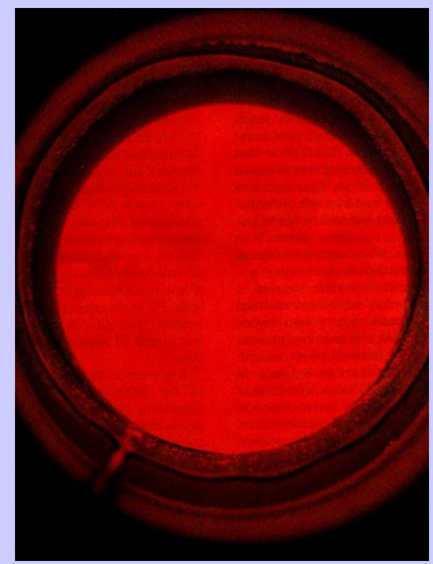

Problems:
η_{EL} < 1% in solid!
η_{PhL}>10%

Bomchil et al., Appl. Surf. Sci., 65/66, 1993

Photoluminescence sensors
Quenching effect

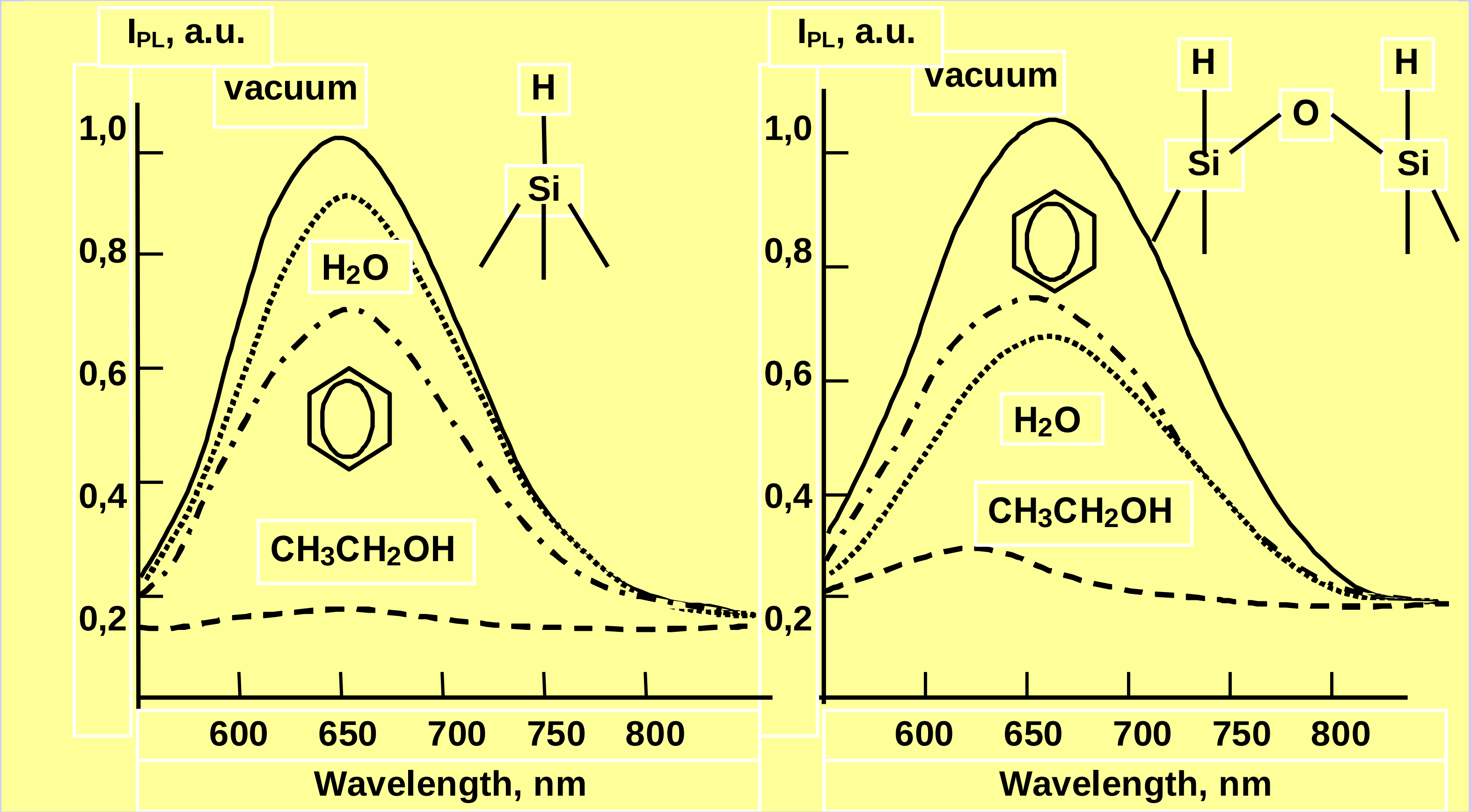

Hydrophobic surface **Hydrophilic surface**

PL spectra of as-prepared (a) and oxidized (b) PS in vacuum, H_2O, benzene, ethanol

/J.M.Lauerhaas, M.Sailor, Science, 261, 1567,1993)/

Photoluminescence quenching

Reversible quenching (physisorbed): alcohols (ethanol, methanol), aromatic (pyrene, anthracenes, benzene, toluene), acid, base….

Irreversible quenching (NO, NO_2, Cl_2, Br_2, I_2, O_2..)
(due to introducing surface non-radiative carrier traps)

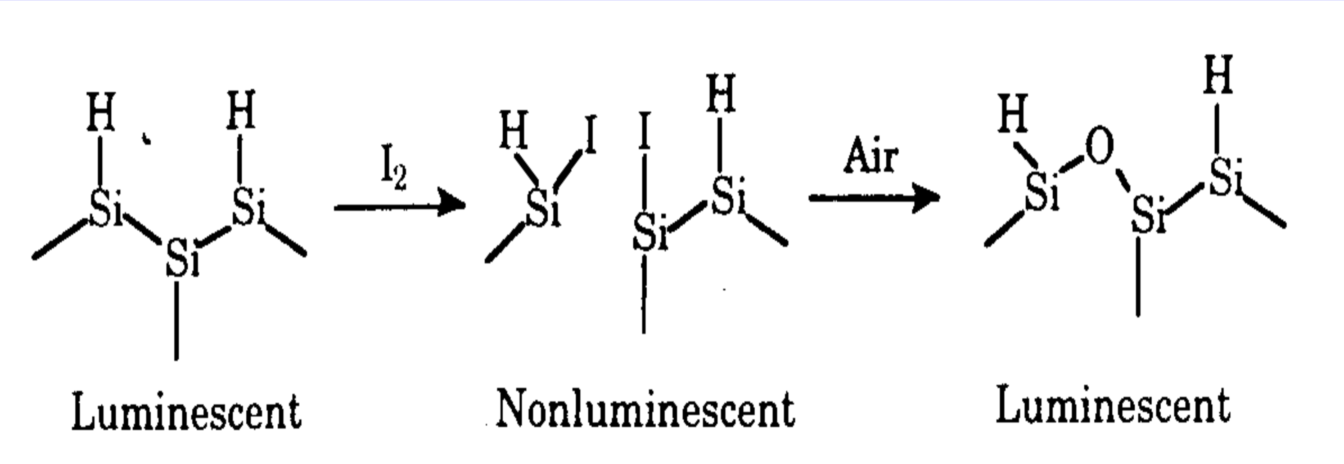

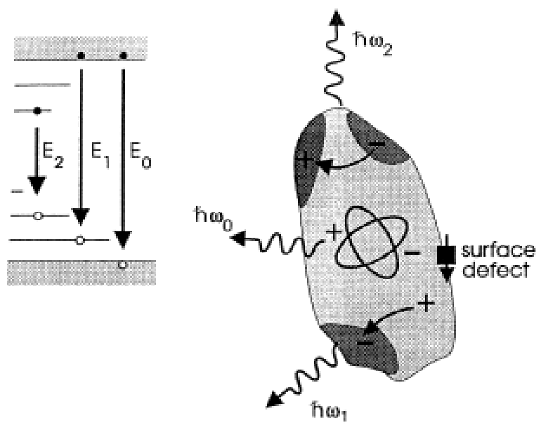

$$\eta_{PL} = \frac{P_{re}}{P_{re} + P_{nre}}$$

Mechanisms of quenching:

- the increase of the non-radiative recombination rate in the nanoparticles due to the alteration of ε
- the change of the nanoparticle electronic structure
- the capture increase on the non-radiative traps at the forming of the strain-induced defects when molecules are adsorbed.

Impact of molecule adsorption on PhL

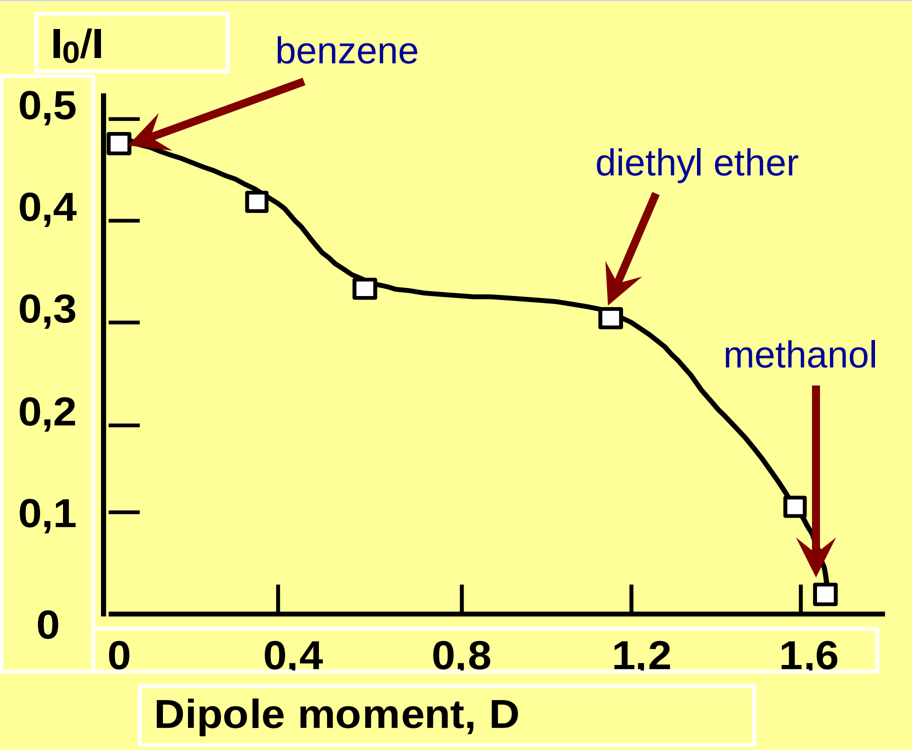

$$p = er$$

PhL intensity versus dipole moment of adsorbates

/J.M.Lauerhaas, M.Sailor, Science, 261, 1567,1993)/

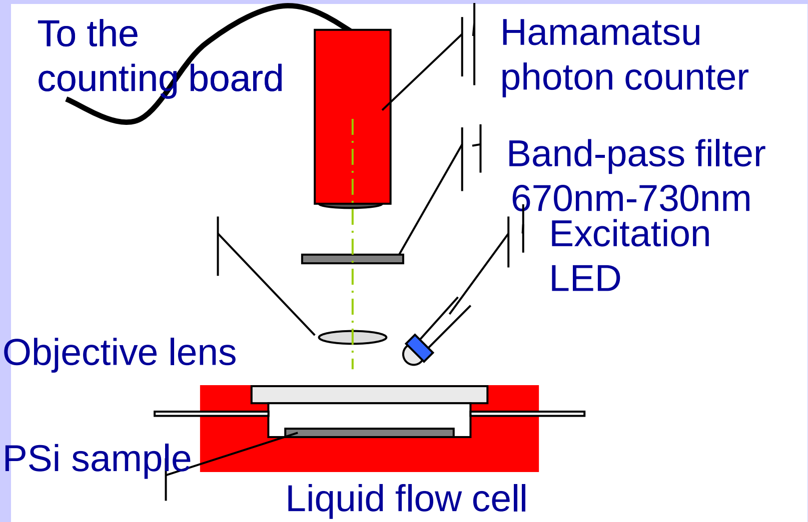

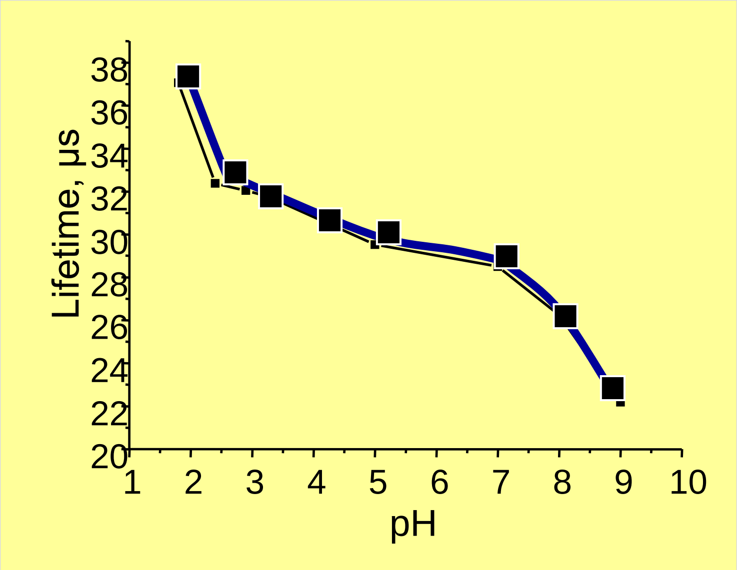

PL decays time versus solution pH

A. Benilov, V. Skryshevsky, Sensors&Actuators, 2007

Optical sensors. Wave guiding

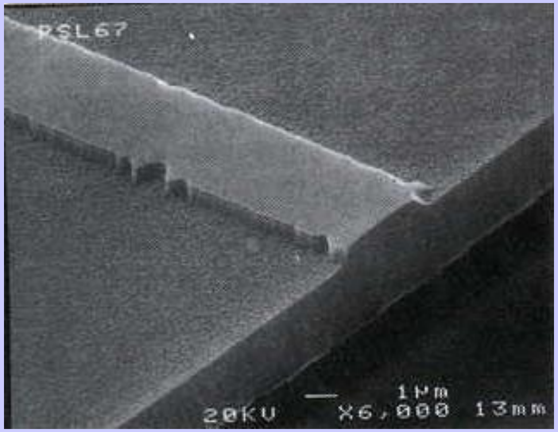

Multilayer Planar Waveguide

G.Loni,Thin Solid Film 276(1996)143

internal reflectance

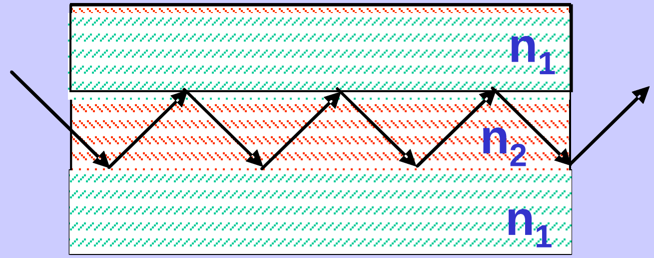

$$n_2 > n_1$$

$$\theta_c = \arcsin\left(\frac{n_2}{n_1}\right)$$

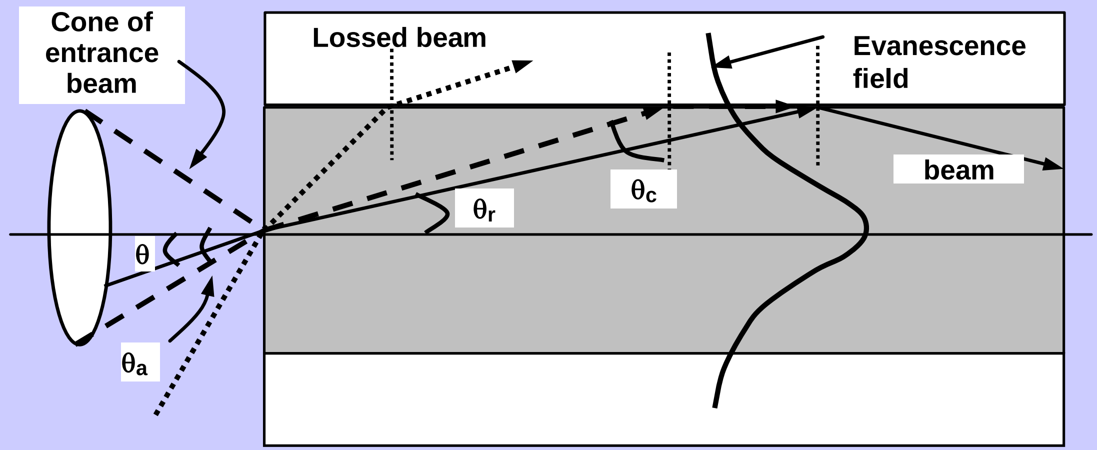

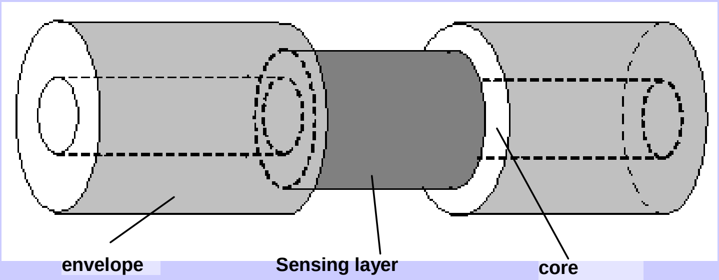

$$d_p = \frac{\lambda}{2\pi\sqrt{(n_1^{\,2}\sin^2\theta_1 - n_2^{\,2})}}$$

Types of optical sensors

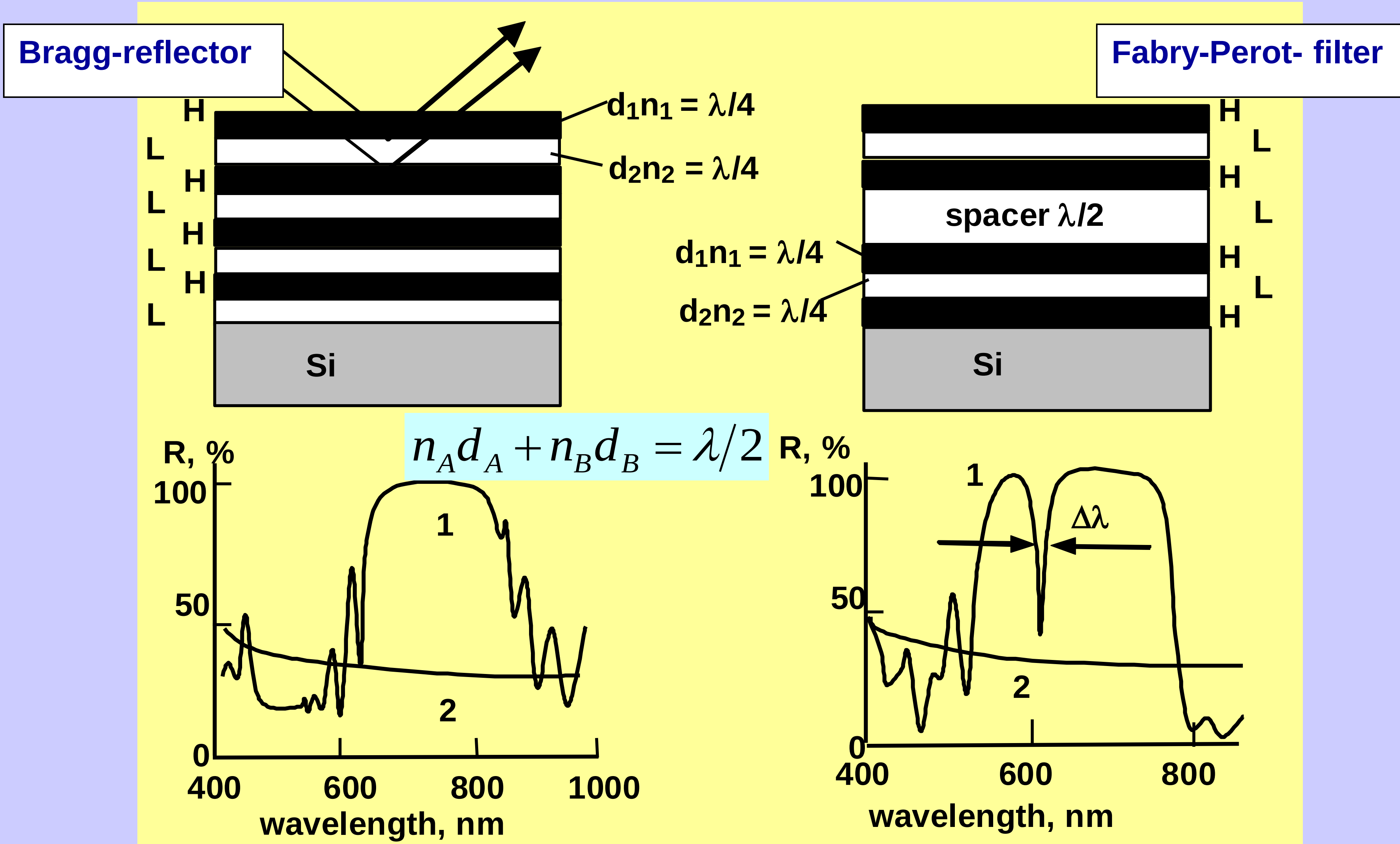

$$n_A d_A + n_B d_B = \lambda/2$$

/M.Thonissen, In: "Properties of porous silicon", ed.L.Canham, Emis, N18, 1997, p.349/

Adsorption in porous silicon

Dipole adsorption – the change of charges on surface states

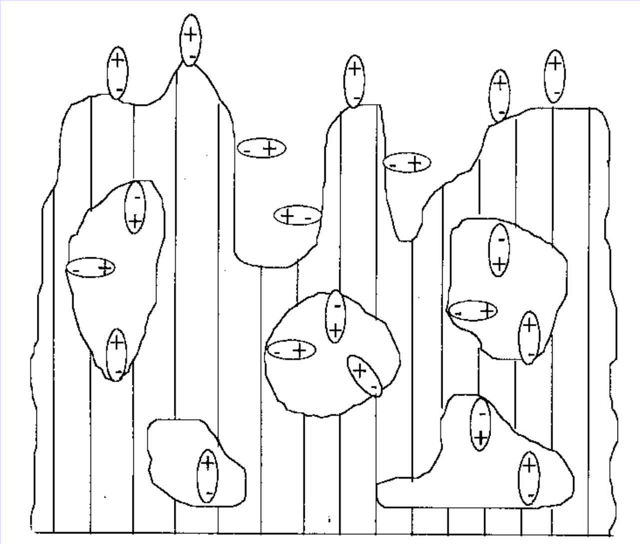

Adsorption of noncharged particules

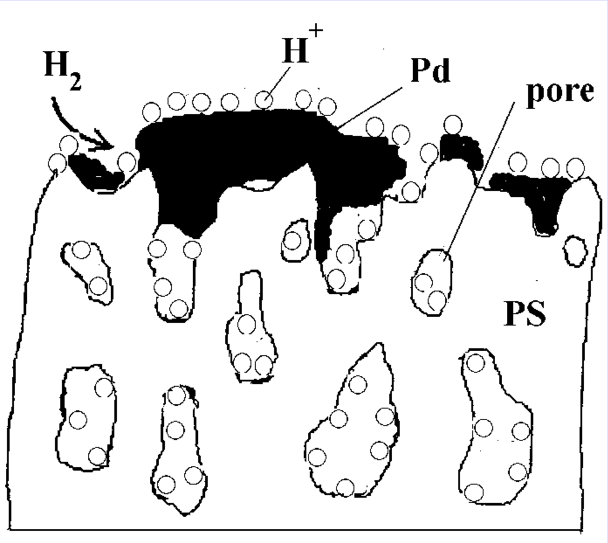

Adsorption in PS: on surface and developed bulk

Porosity: $\mathbf{P=U_p/(U_s+U_p)}$, where $\mathbf{U_p}$, $\mathbf{U_s}$ – volume of pore and Si

Permittivity of PS : $\varepsilon_{PS} = (1-P)\varepsilon_s + P\varepsilon_p$

After adsorption: $\varepsilon_{PSa} = \varepsilon_{PS} + 6P(d_a/d)(\varepsilon_a - \varepsilon_p)$

$$n_{PS} = \sqrt{\varepsilon_{PS}}$$

<u>EXAMPLE:</u> $\varepsilon_{PS} = 5.3$ *for PS (porosity P=0.6, pore diameter d=5 nm)*

After H_2O adsorption ($\varepsilon_a = 80$) ⟹ $\varepsilon_{PSa} = 62$

Optical bio – sensing in microcavity

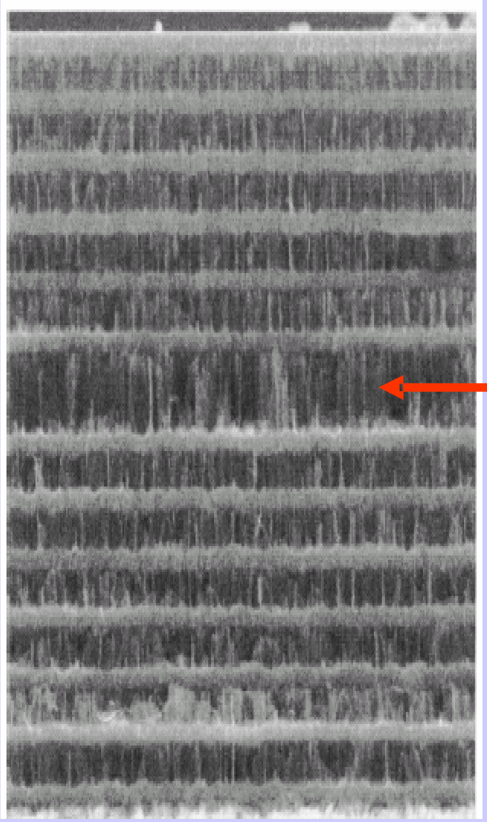

Bragg's mirror

Photoluminescent microcavity

Bragg's mirror

Recognition and binding of bacteriophage lambda DNA

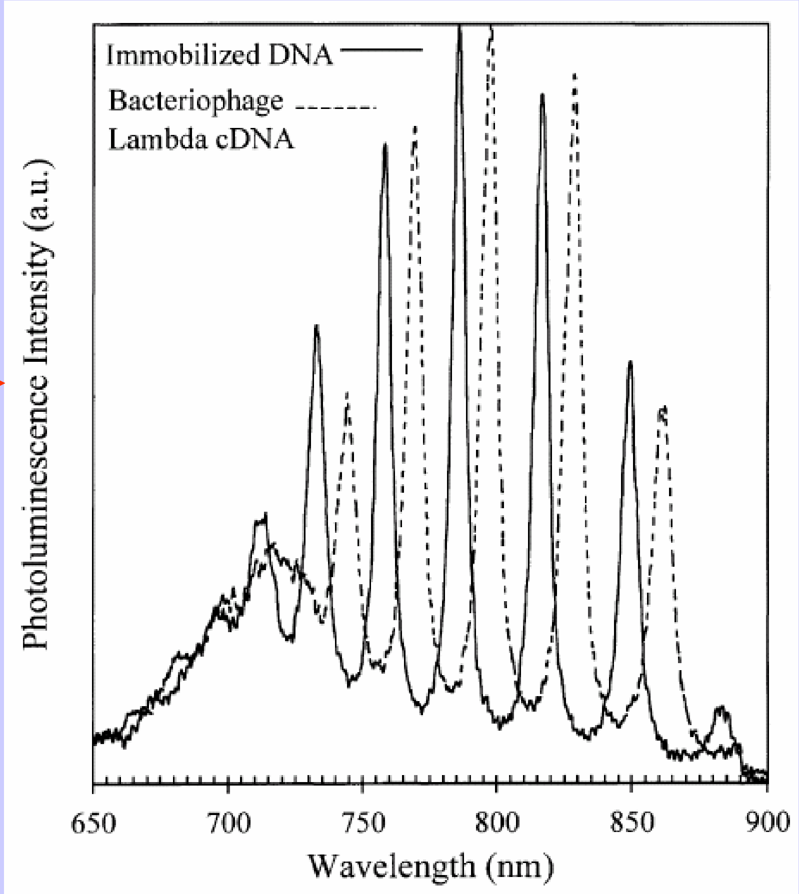

S.Chan et al, Mat.SciEngin,C15(2001)277

Fine tuning of the dichroic behaviour of Bragg reflectors

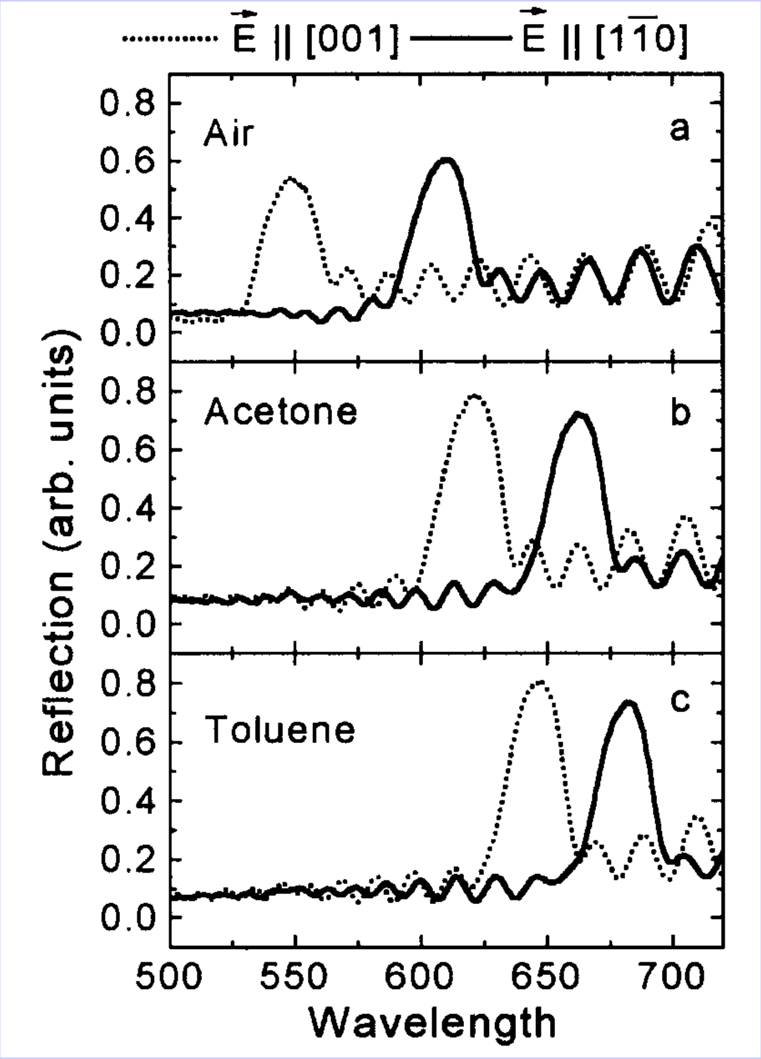

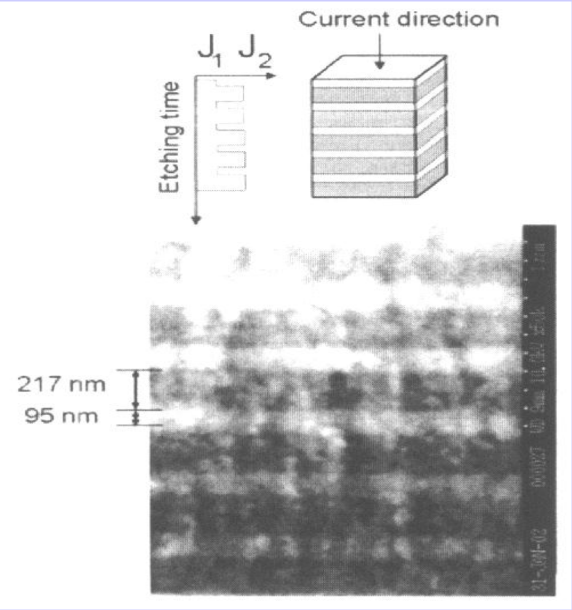

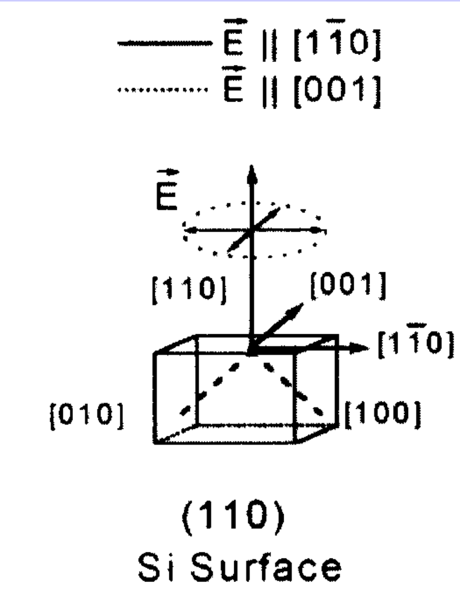

$$n = \frac{1}{2d}\left(\frac{1}{\lambda_r} - \frac{1}{\lambda_{r+1}}\right)^{-1}$$

J.Diener, et al., phys.stat.sol 197 (2003)582

Electrical gas sensing

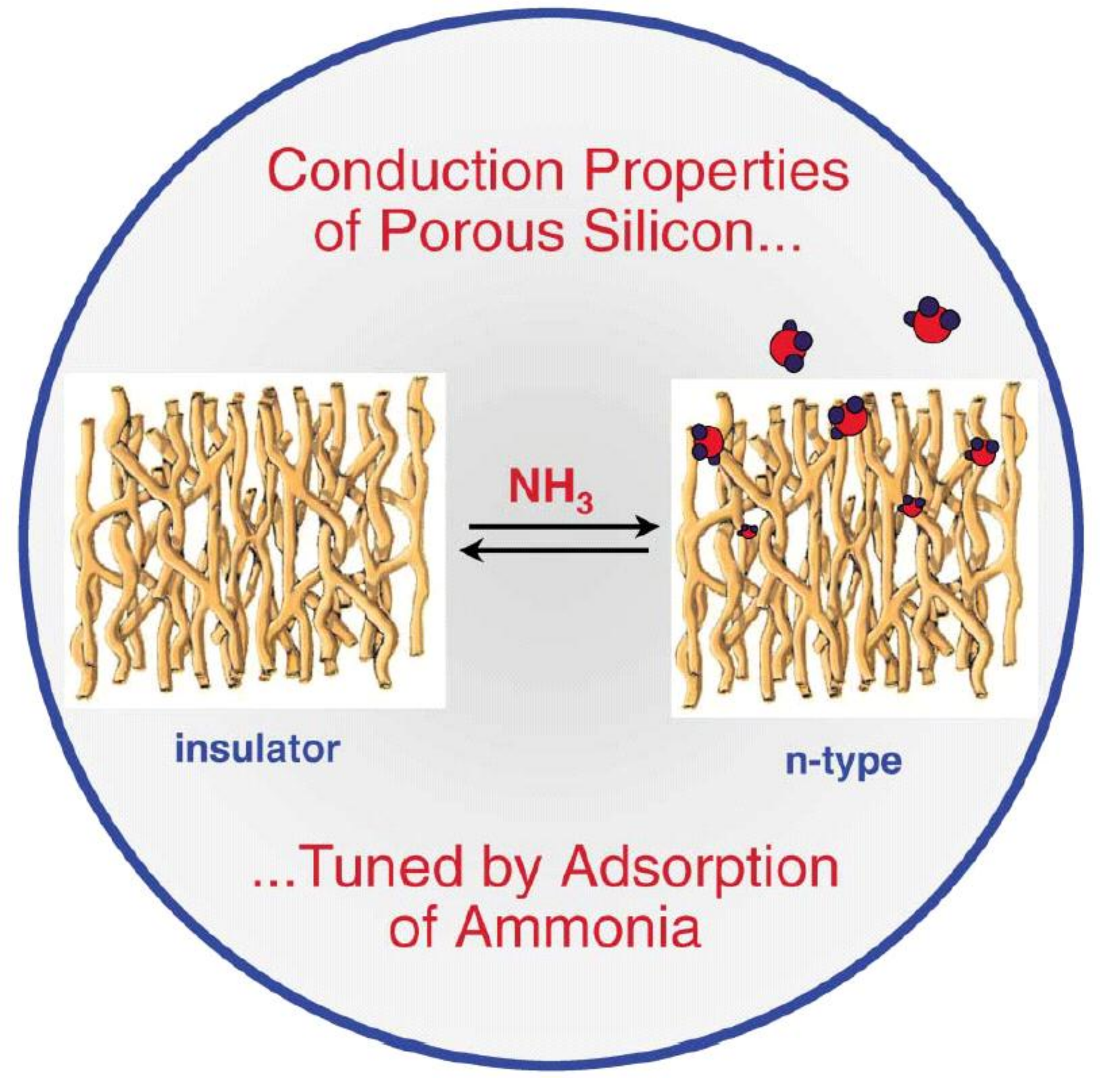

PS Sensor of NO_2

Drude model: $\alpha \sim \lambda^2$

Polarization effect: the induced conductivity at the polar NO molecules adsorption into pores

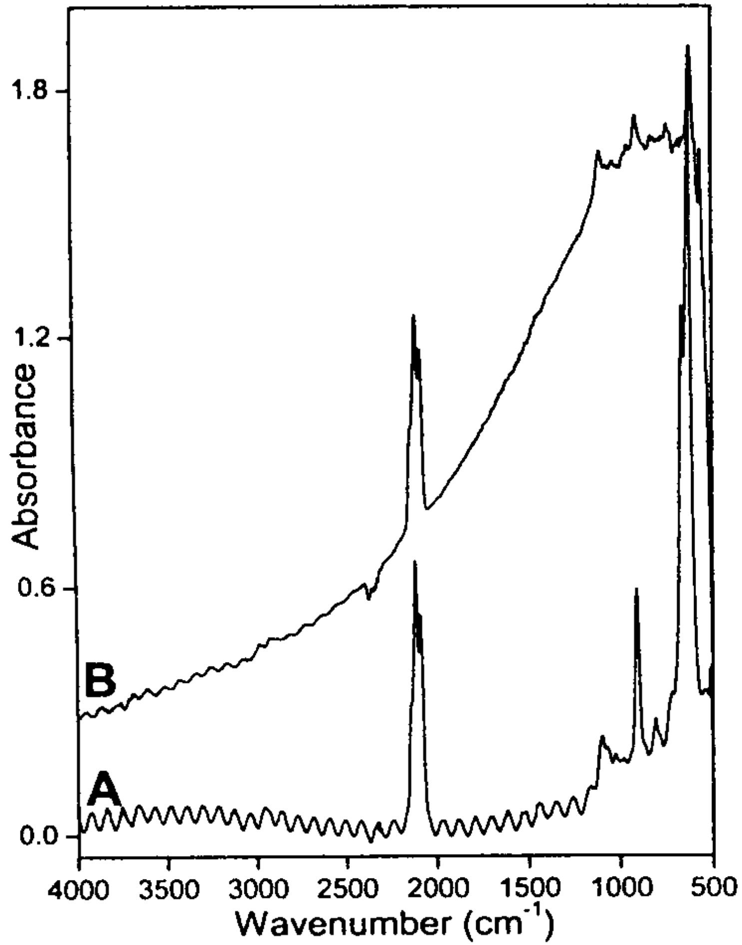

Fig. 1 Infrared absorption spectra. Curve A: PS as-prepared. Curve B: PS in presence of NO_2.

C.J.Oton, et. al., phys.stat.sol, **197** (2003)523

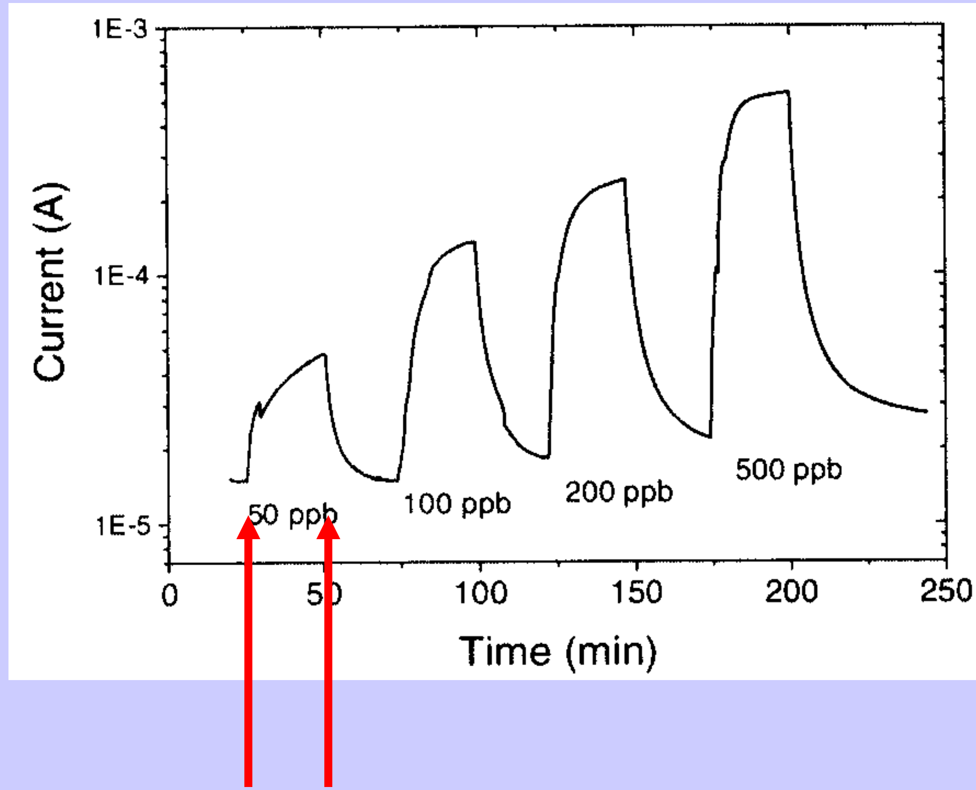

inlet outlet

E.Garrone, et al, phys.stat.sol, **197** (2003)103

Interaction of species at semiconductor surfaces

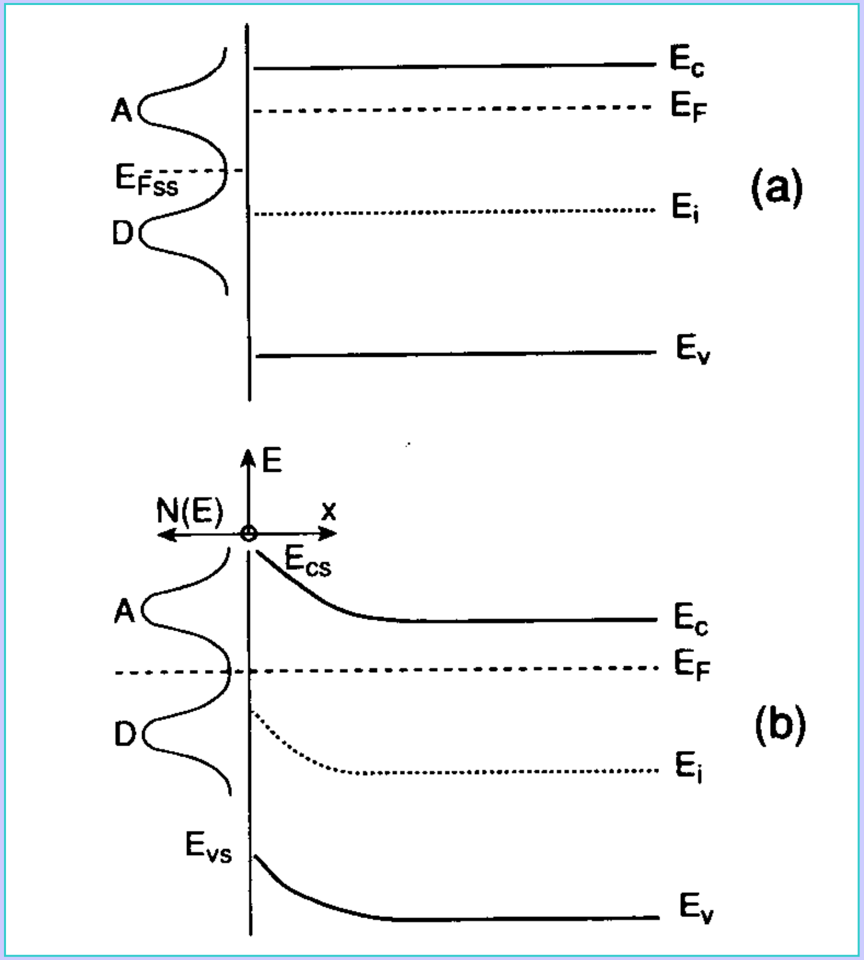

Broken bonds on semiconductor surface form the adsorbing sites for adsorption

Band model of semiconductor surface show the overcharging of surface species:

a- no charge exchange between the semiconductor and surface states;

b- the band bending where e^- from the surface region of semiconductor have moved to surface states to reach equilibrium.

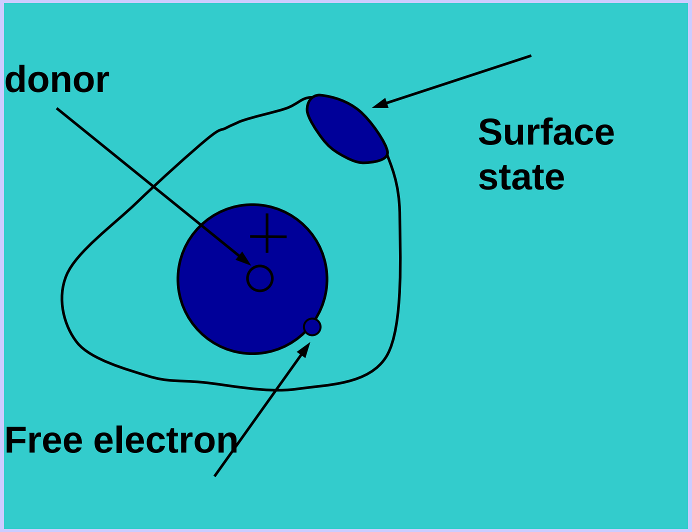

Interaction of gaseous species at semiconductor surfaces

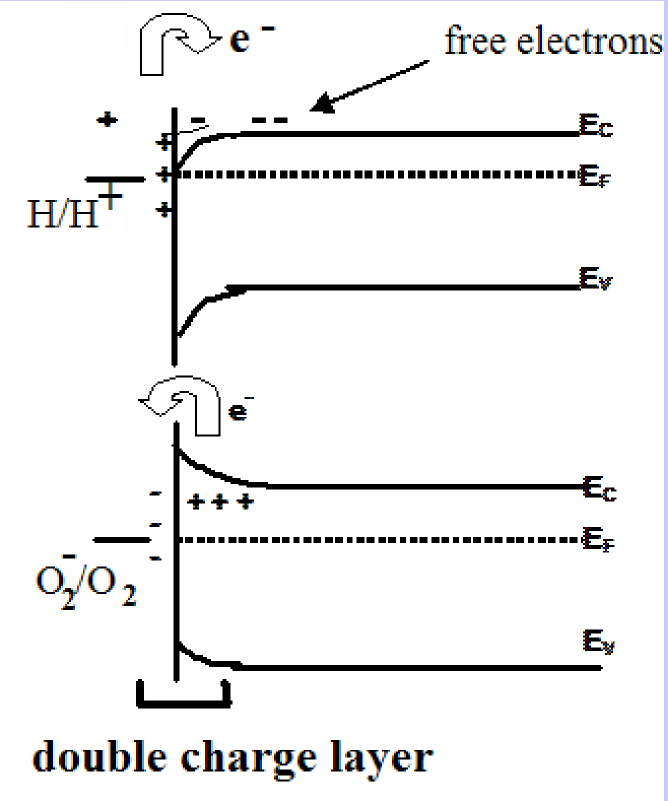

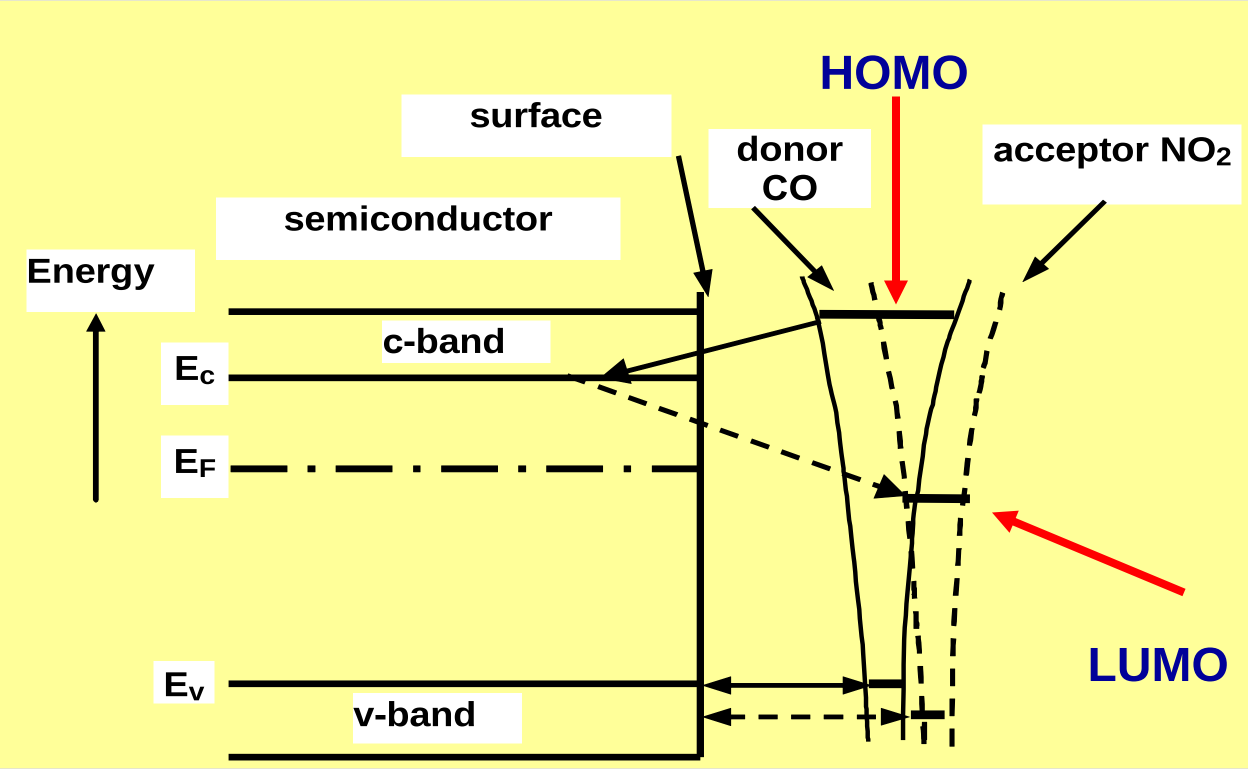

$$C = e\frac{dN}{d\psi} = \frac{\varepsilon\varepsilon_0}{d}$$

The types of adsorbates:

Reducting agents (injection of e^- to bulk):

$H_2 \rightarrow H^+ + H^+ + 2\,e^-$

Oxiding agents (accept of e^- from bulk):

$O_2 + 2\,e^- \rightarrow 2O^-$

Adsorption of molecules in porous materials

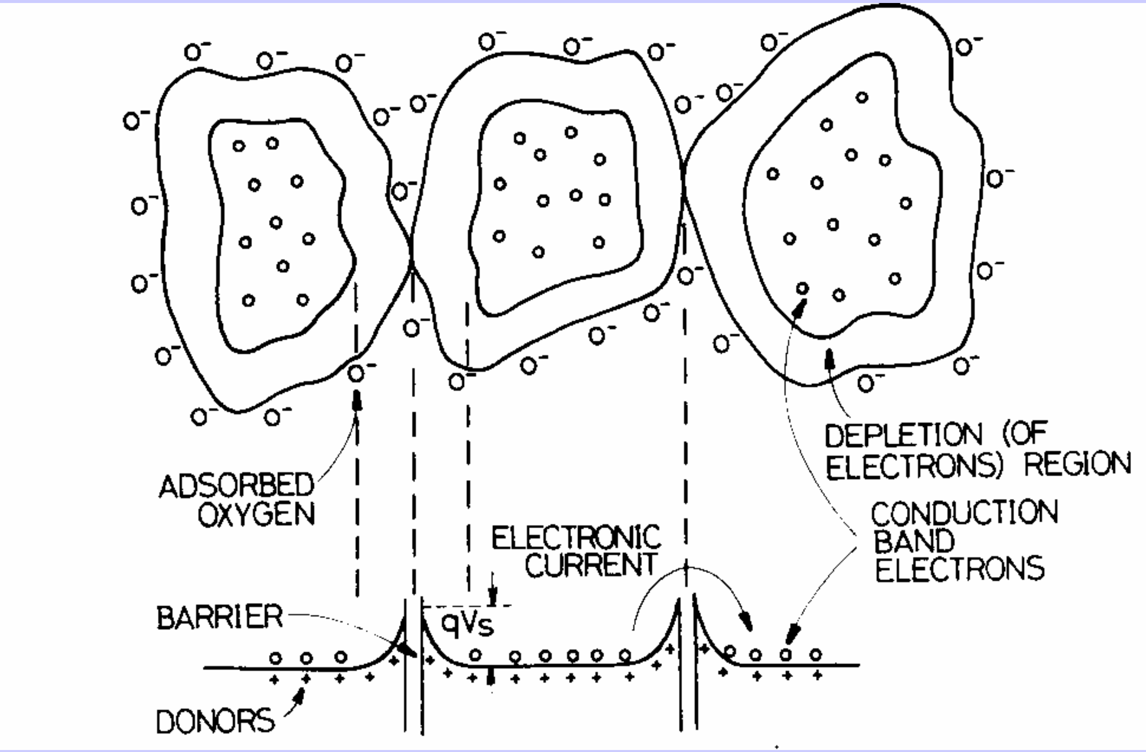

$$\left[O_2^-\right] = N_s = N_D x_0$$

$$e\psi_s = \frac{e^2 N_D}{2\varepsilon\varepsilon_0} x_0^2 = \frac{e^2 N_s^2}{2\varepsilon\varepsilon_0 N_D}$$

$$n_s = N_D \exp\left(-\frac{e\psi_s}{kT}\right)$$

$$G = \frac{1}{R} = G_0 \exp\left(-\frac{e\psi_s}{kT}\right)$$

Adsorption of proton increases the potential barriers between micrograins, adsorption of oxygen decreases these barriers

Porous Silicon Conductivity

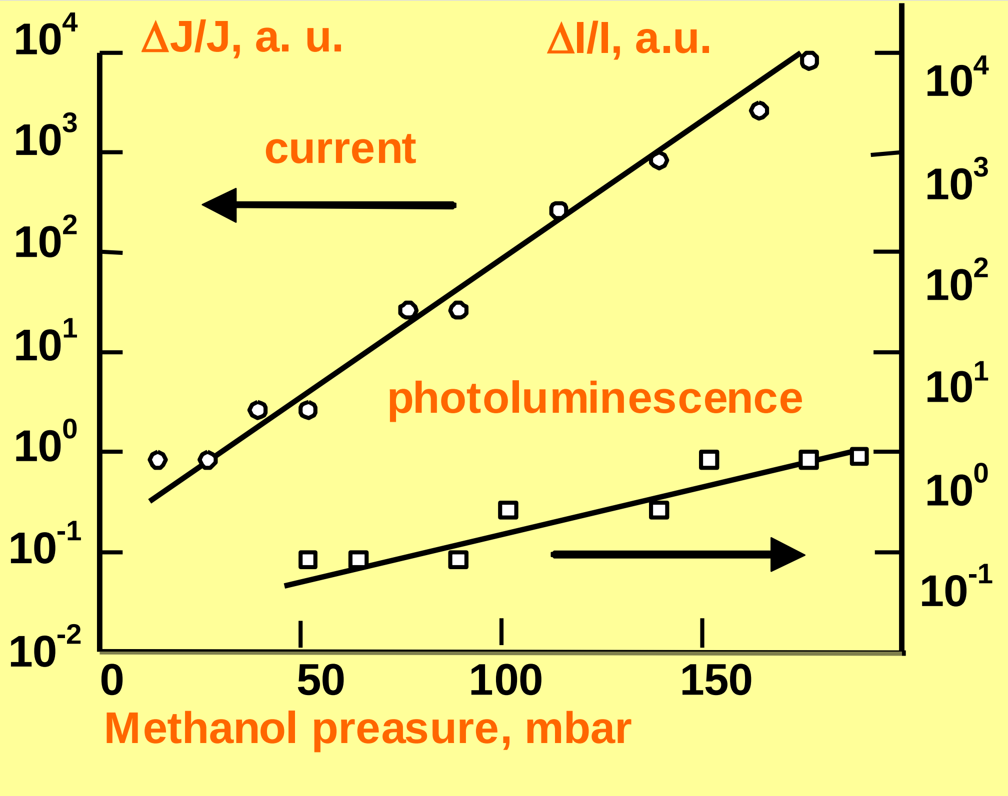

Models for conductivity:

1)the adsorbates make lower the energy barriers between nanoparticles in nanosize Si
2)the change of dielectric constant of nano-Si
3)the charge redistribution inside the nanocrystallites due to the surface states
4)the adsorbates injects extra carriers into nano-Si (reduction-oxidation reactions)

M.Ben-Chorin, A.Kux, I.Schechter, Appl.Phys.Lett, 64, 481 (1994)

2 electrodes transducer

Gold-catalyses PS sensor for NO_x

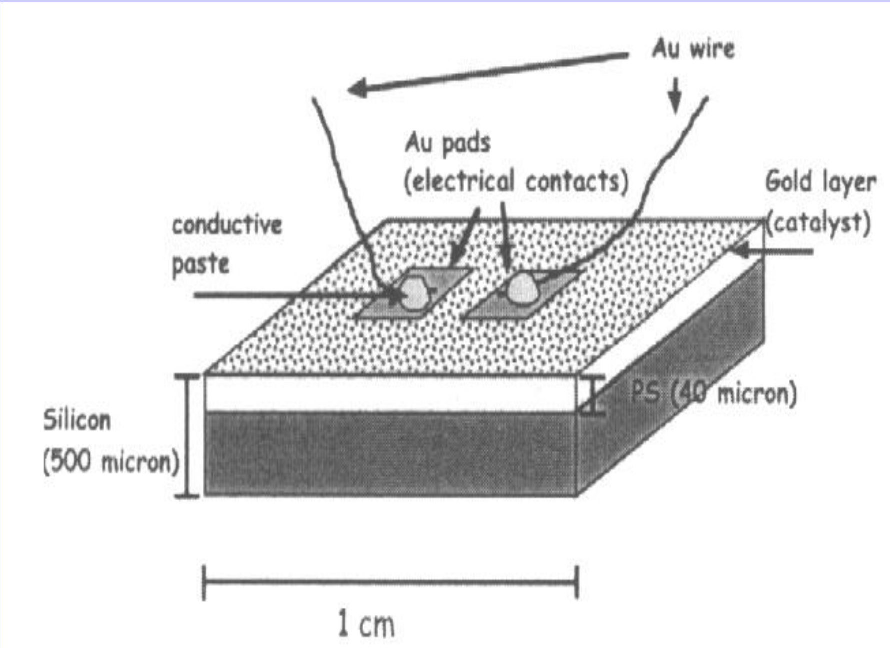

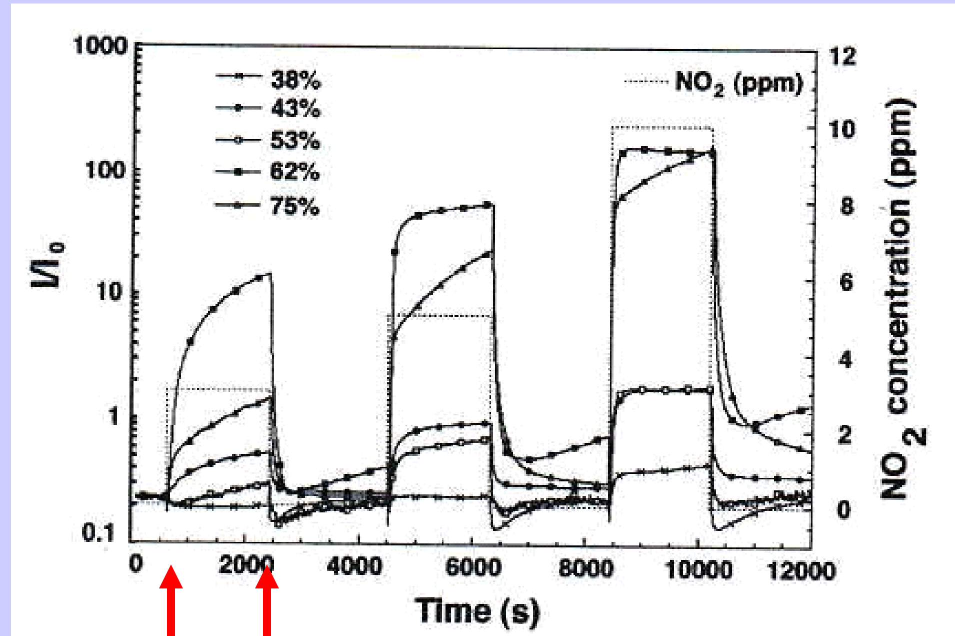

inlet outlet

/C.Baratto, Sensors & Actuators 68(2000)74/

Hydrocarbon sensors with suspended PS membrane

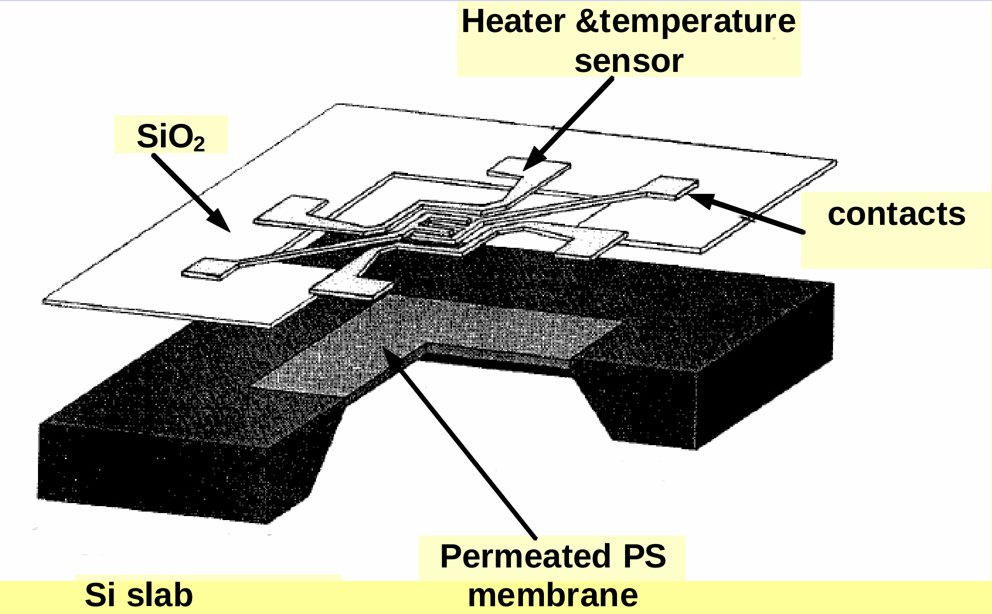

Sensitivity ΔI/I (at 0,5 ppm C_6H_6)	1,0
Response time (90 %), s	80
Recovery time (70 %), s	120
Full time for 1 cycle measurements, min	15
Cross-sensitivity (%) at 1 ppm C_6H_6, 30 ppm CO	30

$$(\Delta I_{C_2H_6+CO} - \Delta I_{CO}) / \Delta I_{C_2H_6+CO}$$

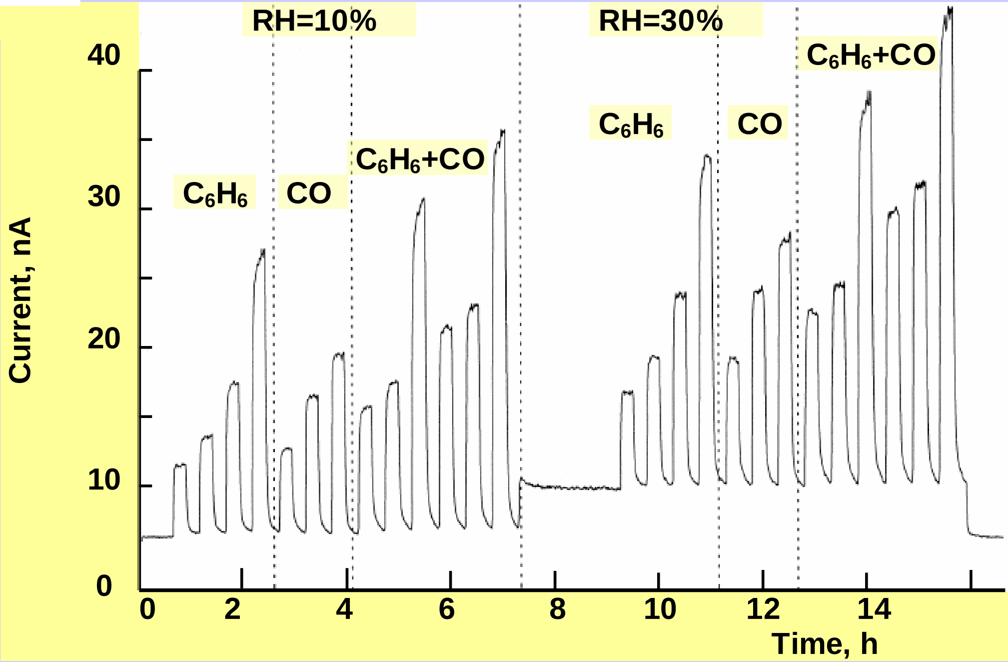

R.Angelucci, Sensors & Actuators, 74(1999)95/

Chemical sensors (H_2) based on FET

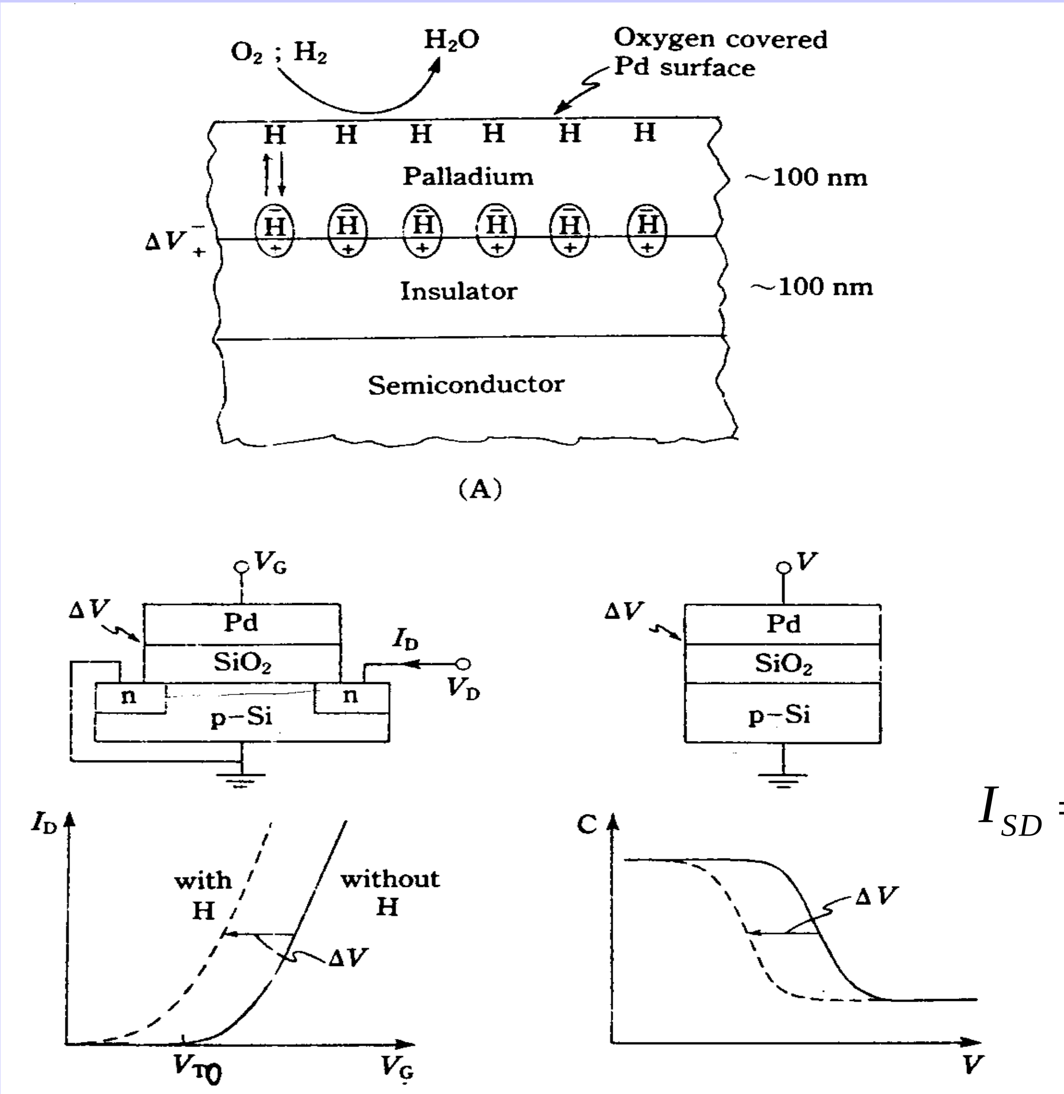

1. Hydrogen adsorption
2. Hydrogen dissociation
3. Penetration of protons through thin Pd film
4. Adsorption as dipole at Pd-SiO_2 interface

$$I_{SD} = \mu_n C_{ox} \frac{W}{L}\left[(V_G - V_T)V_{SD} - \frac{V_{SD}^2}{2}\right]$$

$V_T = V_{T0} - \Delta V$

$\Delta V = -\mu N_s \theta / \varepsilon_0$

Lundstrom I. *Sensors and Actuators*, 1 (1981) 403.

FET sensor (alcohol, acids) and capacity

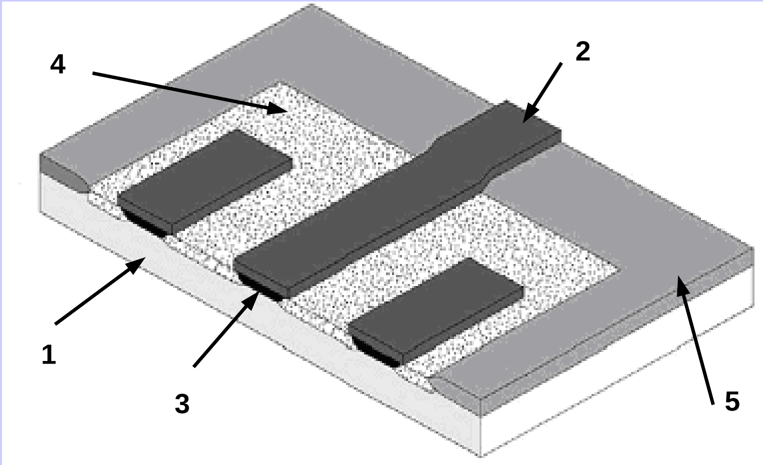

1- p-Si (10^{15} cм$^{-3}$), 2- n^+ -Si, 3- impl. n-Si ($4x10^{20}$ cм$^{-3}$), 4- PS, 5- Si_3N_4

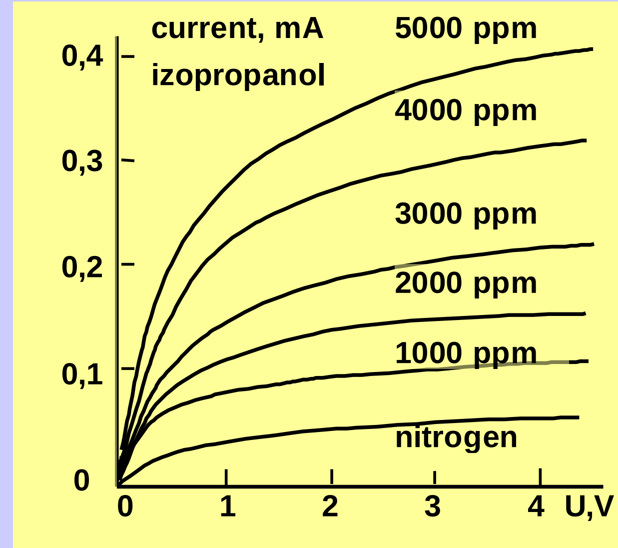

/G.Barillaro, Sensors & Actuators, 2003/

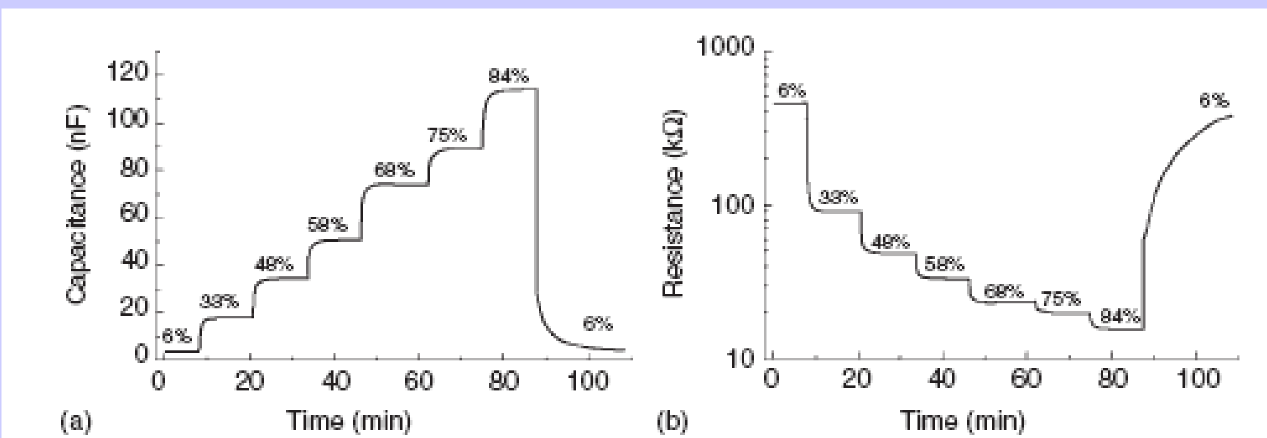

Figure 4.11 Dynamic response of (a) the capacitance and (b) the resistance of a TC-PS humidity sensor. Corresponding RH values are shown in the figures. Electrical parameters were measured using an 85 Hz frequency [58].

Sensor based on CMOS process

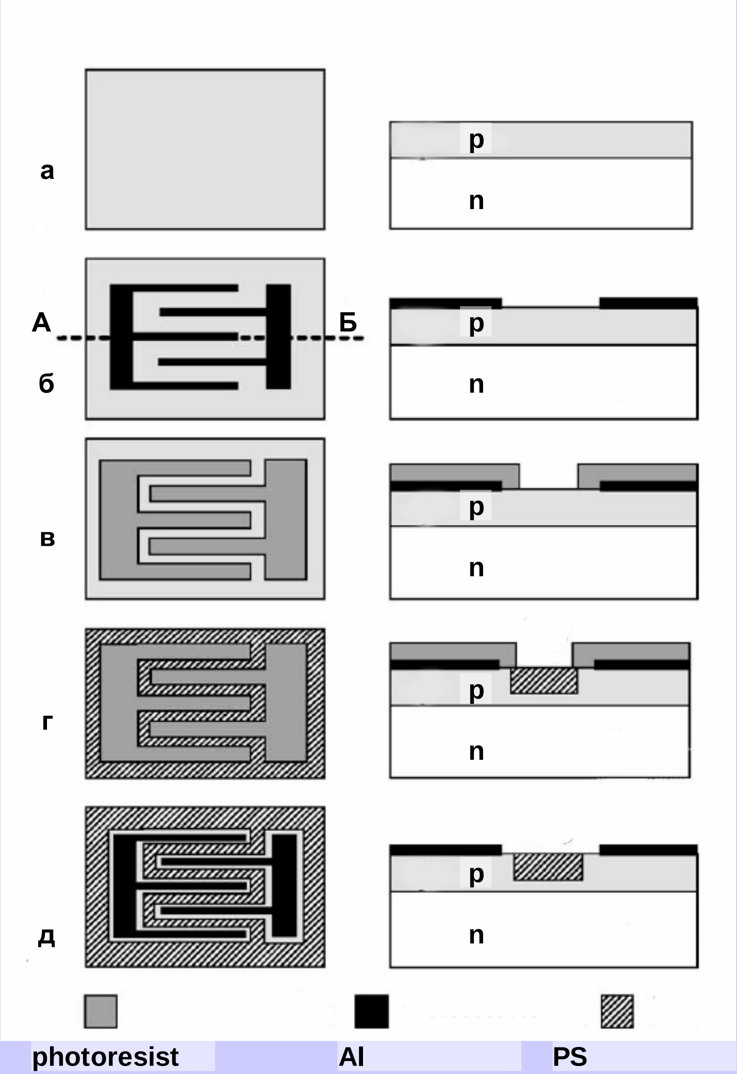

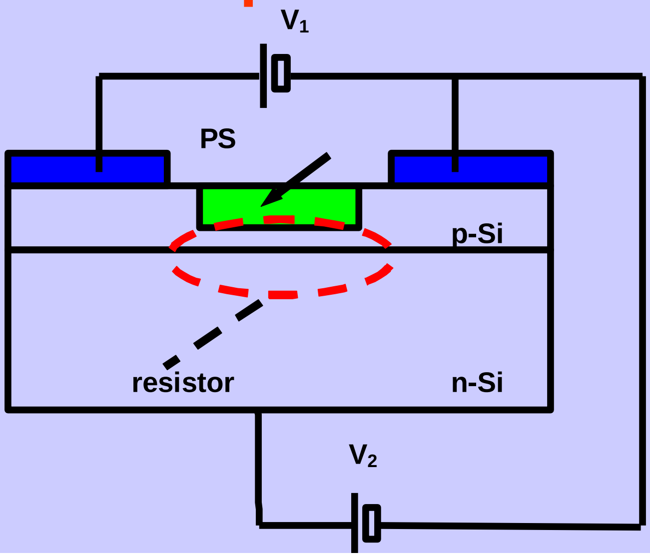

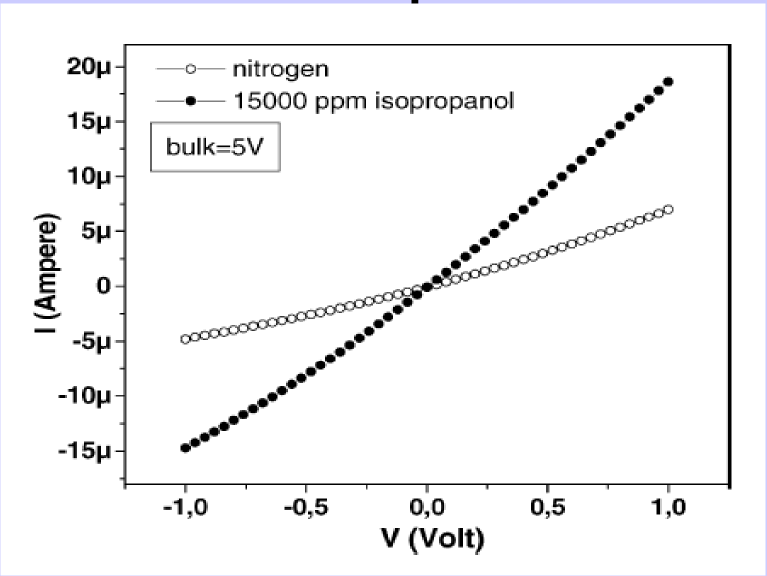

G.Barillaro, et al Sensor & Activators, B, 2004

Hydrogen storage in PS

$$N_H = \frac{1}{\Gamma_S \rho_{Si}(1-P)} \int_{h\upsilon} \frac{\alpha}{h\upsilon} d(h\upsilon) = \frac{I_S}{\Gamma_S \rho_{Si}(1-P)}$$

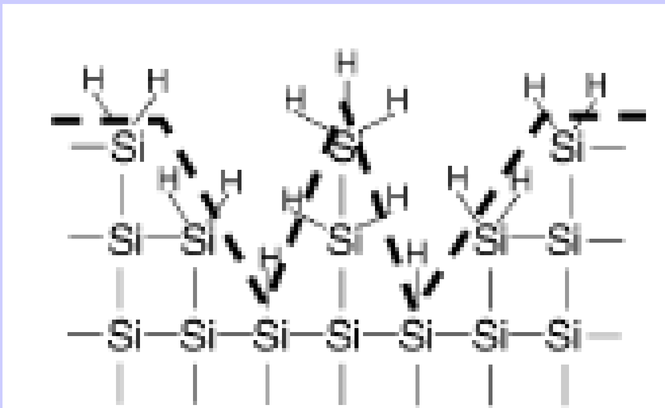

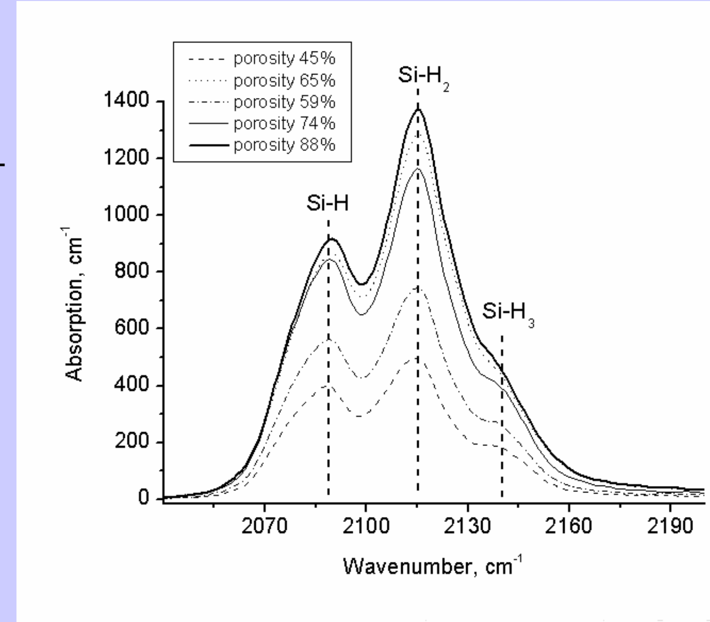

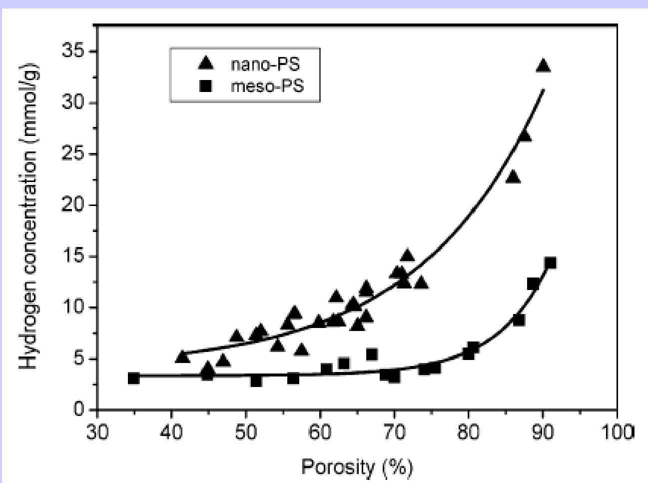

Hydrogen concentration in atomic, C_H (at.%), or mass C_M (mass%):

$$C_H = \frac{m_{Si} N_H}{1000\rho_{Si}(1-P) + N_H(m_{Si} - m_H)}$$

$$C_M = \frac{1}{1 + \frac{m_{Si}}{m_H}\left(\frac{1}{C_H} - 1\right)}$$

Reduction of Si nanoparticles dimension sharply increases the hydrogen concentration in PS.

Lysenko V., Barbier D., Skryshevsky V., et al., Appl.Surf.Sci., 230(2004)425

Hydrogen storage in PS

TABLE 1: Comparative Energetic Analysis of PS Nanostructures for Their Application as Hydrogen Reservoirs in Portable Devices

materials	atomic hydrogen content, (mmol g^{-1})	theoretical mass energy density, (W-h kg^{-1})	autonomy (h) of a device consuming 1 W and using 100 g of material storing hydrogen *(taking into account 50% efficiency of low-temperature fuel cell)*
meso-PS (90%, 10 nm)	13	429	21.4
nano-PS (90%, 5 nm)	34	1120	56.1
nano-PS powder (>95%, 2−3 nm)	66	2176	108.8
reversible metal hydrides[4]			
$MgH_2 \rightarrow Mg + H_2$	76	2505	125.2
$LaNi_5H_6 \rightarrow LaNi_5 + 3H_2$	14	461	23
hydride hydrolysis[4]			
$(NaBH_4 + 2H_2O) \rightarrow NaBO_2 + 4H_2$	108	3560	178
$(LiBH_4 + 4H_2O) \rightarrow LiOH + H_3BO_3 + 4H_2$	85	2802	140.1
hydride thermolysis[4]			
$NH_4BH_4 \rightarrow BN + 4H_2$	244	8043	402.1
$NH_3BH_3 \rightarrow BN + 3H_2$	195	6428	321.4
methanol reforming			
$(CH_3OH + H_2O) \rightarrow CO_2 + 3H_2$	120	3956	197.8
Li-ion batteries (24)[5] (for comparison)		150	15

2 mmol/g (H_2, 60% porosity)

3,7 mmol/cm^{-3} (H)

(Rivolo et al., Phys. Stat. Sol. (a) 197, (2003) 217)

Nano-porous powder, nanocrystallite dimension - 2nm → **66 mmol/g H**

Hydrogen storage in PS

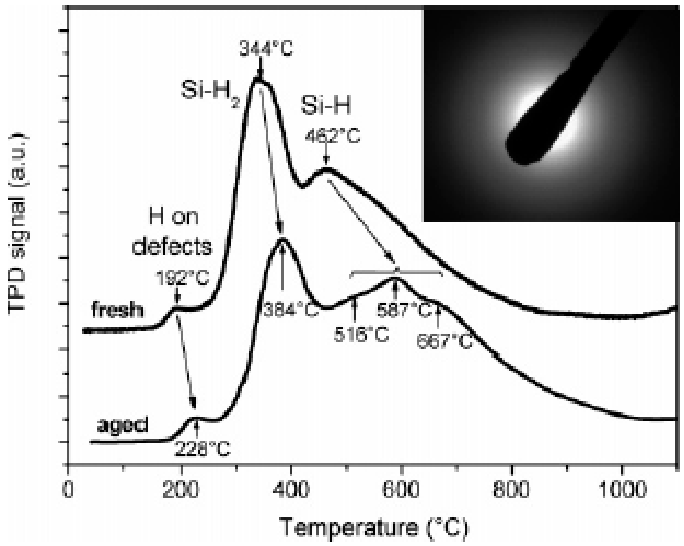

Figure 6. Effusion curves for H_2 desorption from fresh and aged nano-PS samples. Electron diffraction image given in insert reflects amorphous structure of the PS samples.

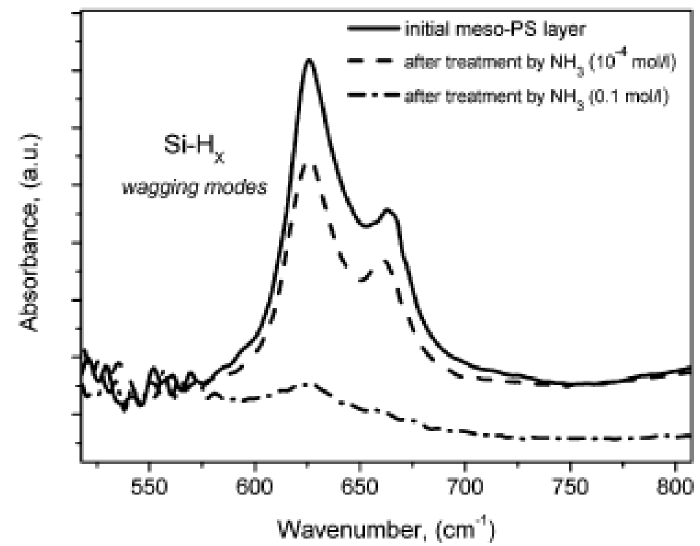

Figure 7. Chemically stimulated desorption of hydrogen from meso-PS layers. IR absorption spectra of Si$-$H$_x$ wagging band corresponding to the hydrogenated meso-PS layers treated by NH_3 solutions.

Thermally stimulated desorption

Chemically stimulated desorption

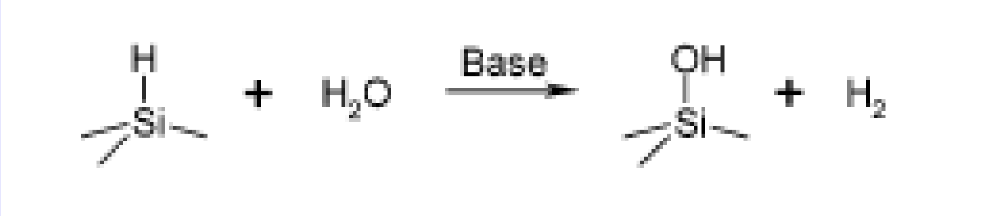

V.Lysenko, et.al. J.Phys.Chem., B, 2005, 109, 19711

Portable energy supply

1 W

+ 10g of nano-porous *(6.6 wt%)* → **11 hours of autonomy** *(Li battery: 1 hour)*

V.Lysenko, private commun.

Thermal isolation

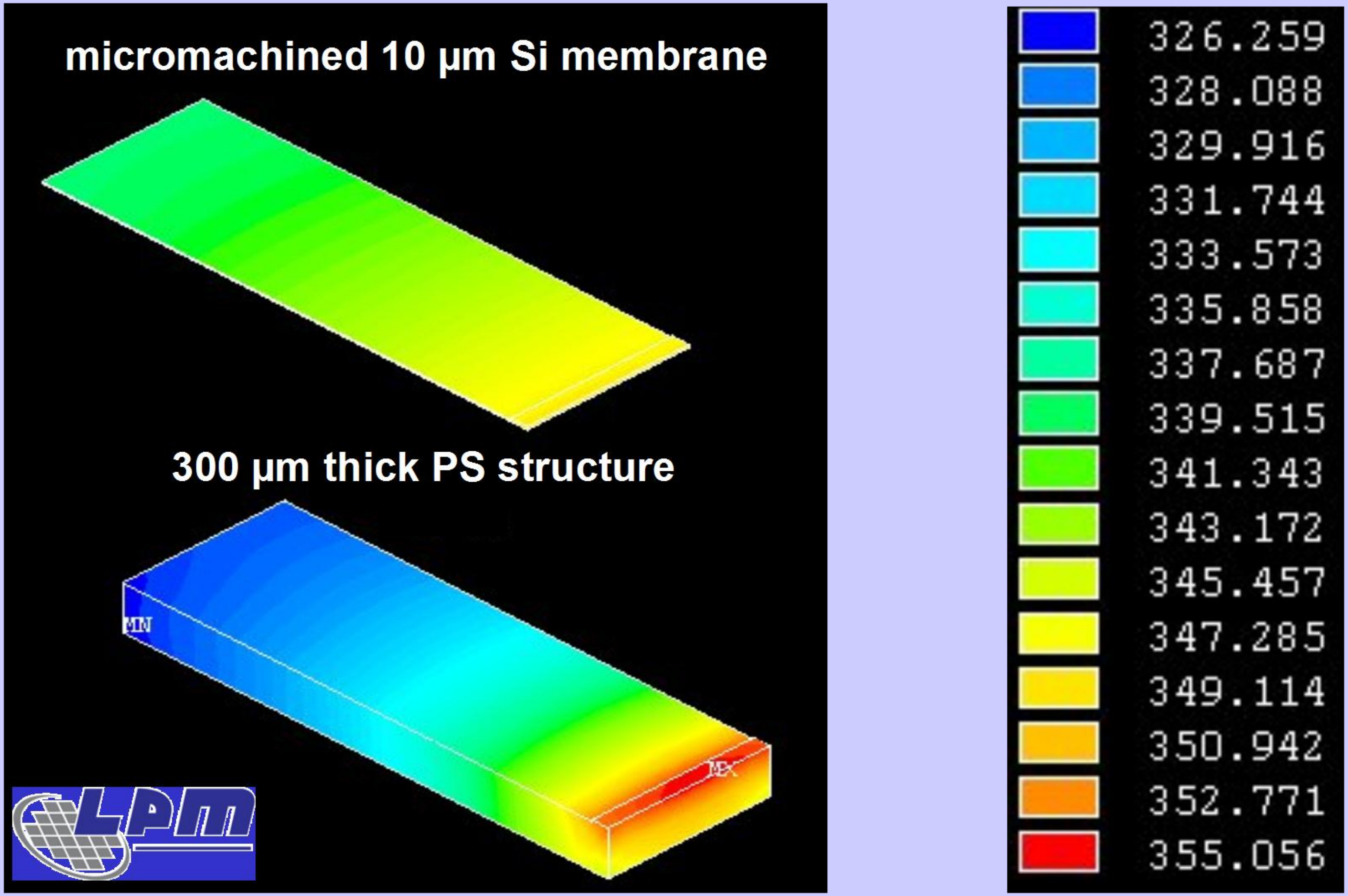

Explosive reactions

- Conditions: H-terminated porous Si surface + liquid oxygen
- 3 step chain mechanism : a) oxidation of Si dangling bonds (10^{16} cm^{-3});
  b) rupture of Si-H bonds;
  c) $2H_2+O_2=2H_2O$ ...

- Energy yield : 12- 28 kJ/g
  (trinitrotoluene : 4.2 kJ/g)
- Explosion time : $2x10^{-7}$ s
- Velocity of the reaction front propagation : 10^4 m/s
- Shock wave pressure : 11 GPa/cm^2

Kovalev et al., Phys. Rev. Lett. 87, (2001) 068301

Table 19.2 Overview of some thermodynamic reaction parameters for several mixtures of Si with oxidizer.

Chemical reaction equations	ΔH_r^0 (kJ)	ΔH_r^0 (kJ/g)	T_{rct} (K)
$Si + O_2 \rightarrow SiO_2$	−911	−15.2	3131
$4Si + Ca(ClO_4)_2 \rightarrow 4SiO_2 + CaCl_2$	−3703	−10.5	3093
$2Si + NaClO_4 \rightarrow 2SiO_2 + NaCl$	−1850	−10.4	3057
$2Si + KClO_4 \rightarrow 2SiO_2 + KCl$	−1825	−9.4	3061
$5Si + 4NH_4ClO_4 \rightarrow 5SiO_2 + 2N_2 + 4HCl + 6H_2O$	−5453	−8.9	2917
$5Si + 4NaNO_3 \rightarrow 5SiO_2 + 2N_2 + 2Na_2O$	−3519	−7.3	2893
$5Si + 4KNO_3 \rightarrow 5SiO_2 + 2N_2 + 2K_2O$	−3305	−6.1	2980
$4Si + S_8 \rightarrow 4SiS_2$	−848	−2.3	1759
$nSi + (C_2F_4)_n \rightarrow nSiF_4 + 2nC$	−798	−6.2	3532

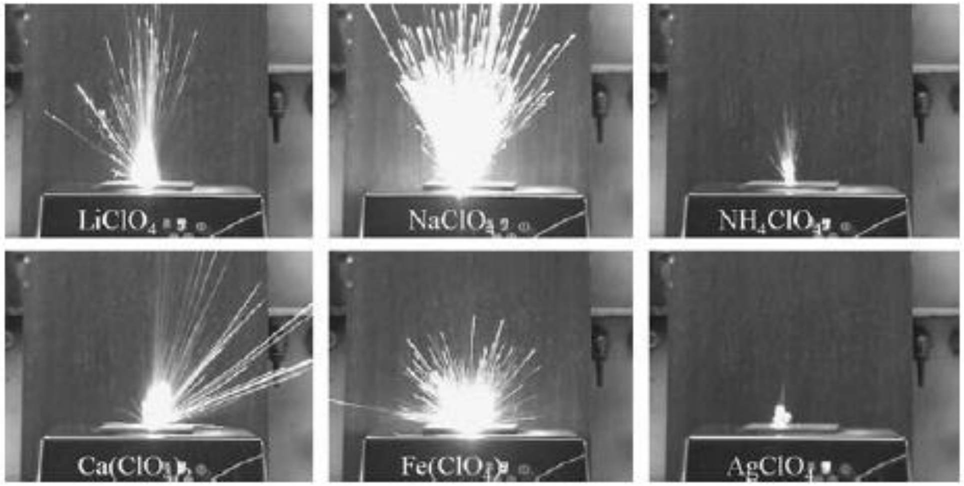

Figure 19.14 Time-integrated flame pictures of 3 × 3 mm PSi single elements filled with the indicated oxidizers (this image was prepared by D. Clément, Technical University of Munich, for the "SilAnz" report [14]).

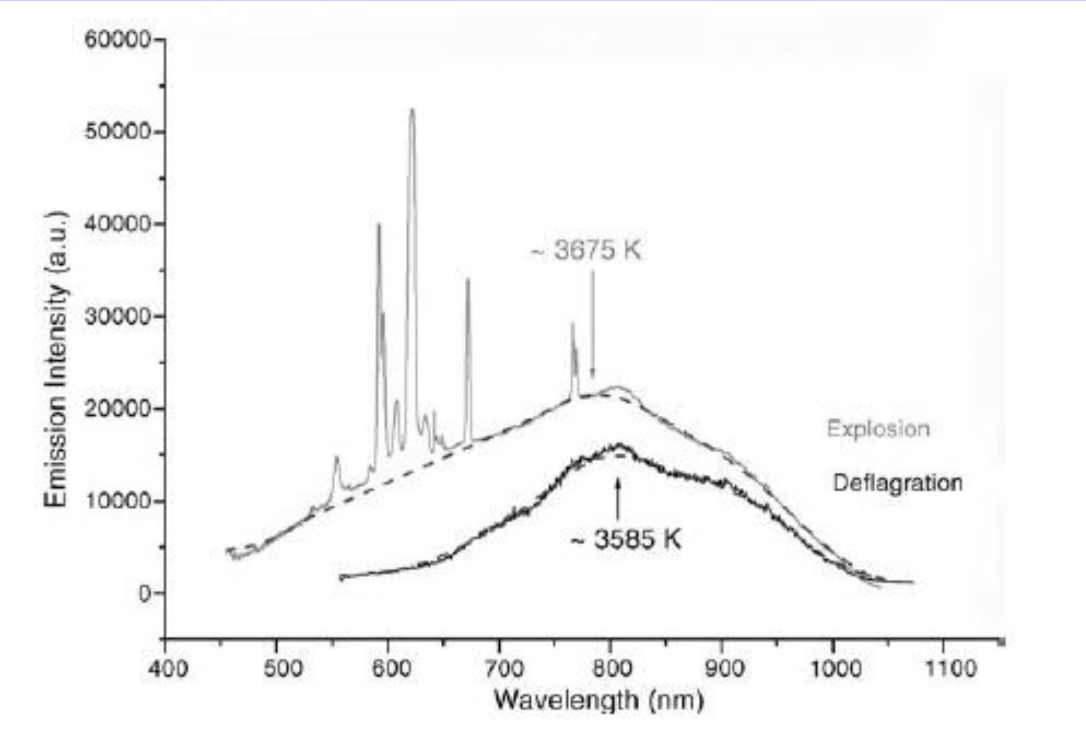

Figure 19.13 Emission spectra of flashes accompanying the explosions. The reaction temperatures are indicated and were estimated by the approach of a blackbody emission. They are very similar for the deflagration and the explosion. The spectrum of the explosion additionally shows the appearance of plasma lines of single or double ionized atoms demonstrating the presence of hot spots having temperatures much higher than the estimated ones (this image was prepared by D. Clément, Technical University of Munich, for the "SilAnz" report [14]).

Biosilicon ™

(pSi Medica Ltd., Prof. L. Canham)

"Intelligent" tablets releasing the drugs when and where they are needed.

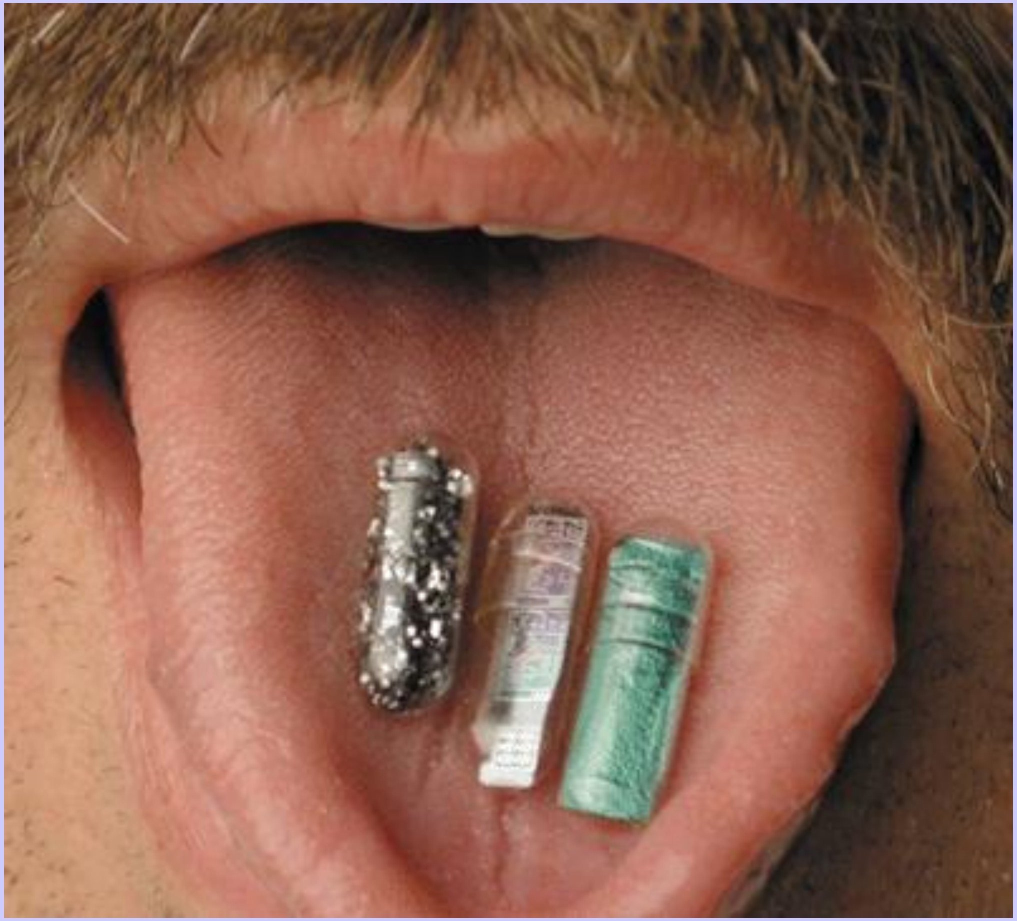

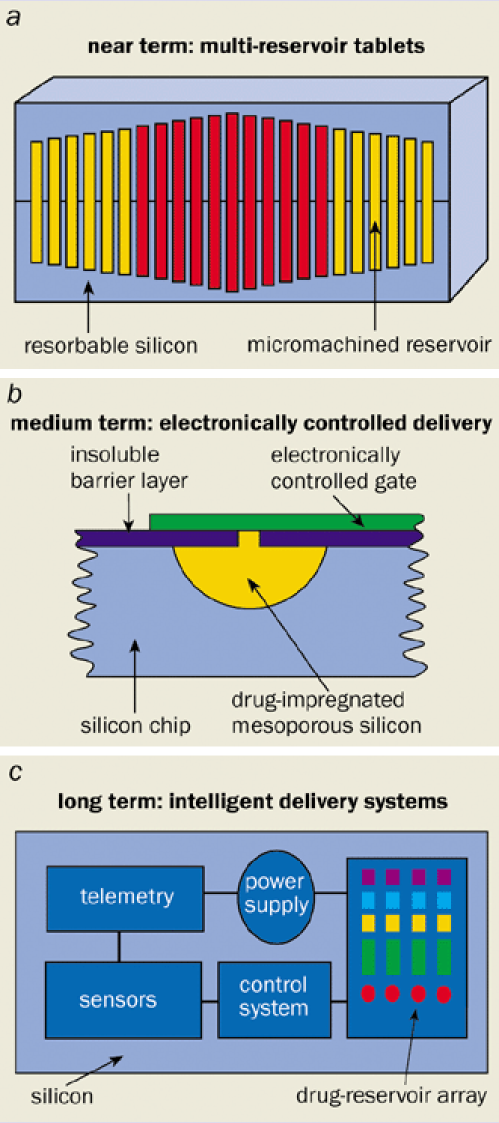

Drug delivery with magnetic nanoparticles in porous silicon

Figure 1 Tiny reactors. Drops of aqueous solutions of Ag^+ and I^- in dichloromethane are coated with a self-assembled layer of magnetic porous silicon crystals. The droplets are transported with magnets towards each other. When they meet they coalesce to form a new, larger droplet. The precipitation of insoluble AgI takes place immediately inside the newly merged aqueous drop.

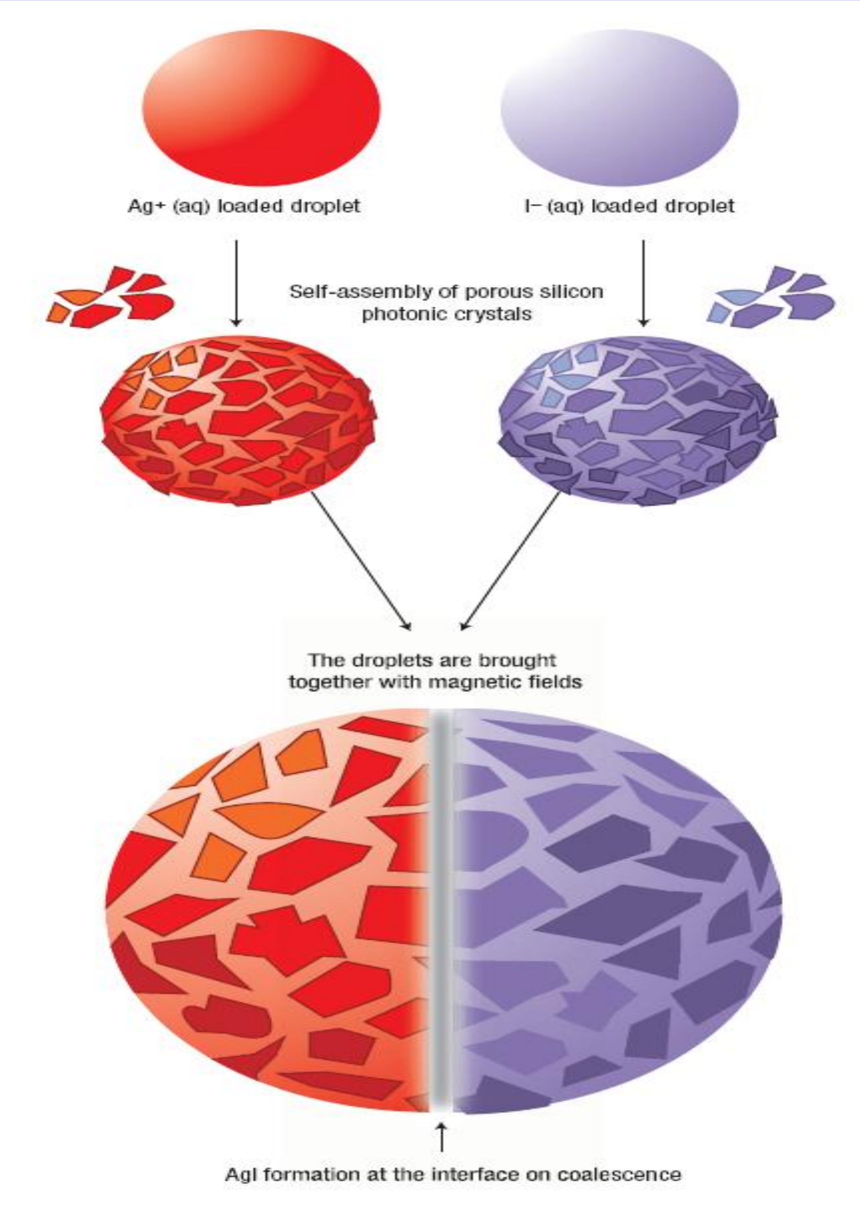

J.Buriak, Nature materials, 3, 2004, 847

SiC NPs as a contrast and fluorescent agent for animal cells imaging

FIBROBLAST CELLS

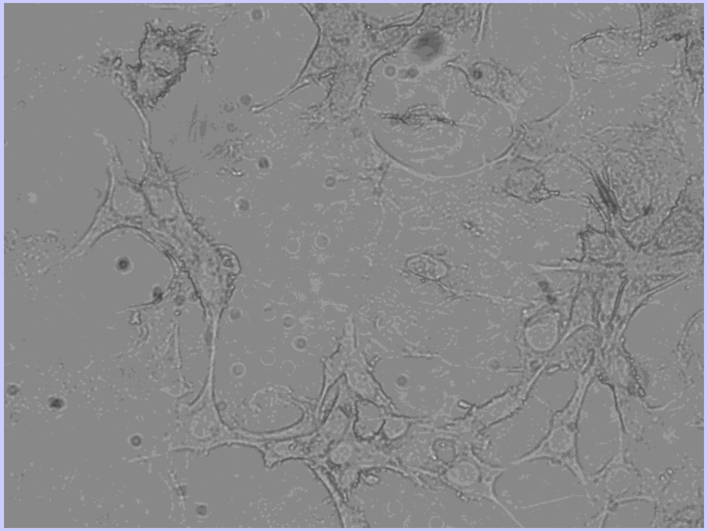

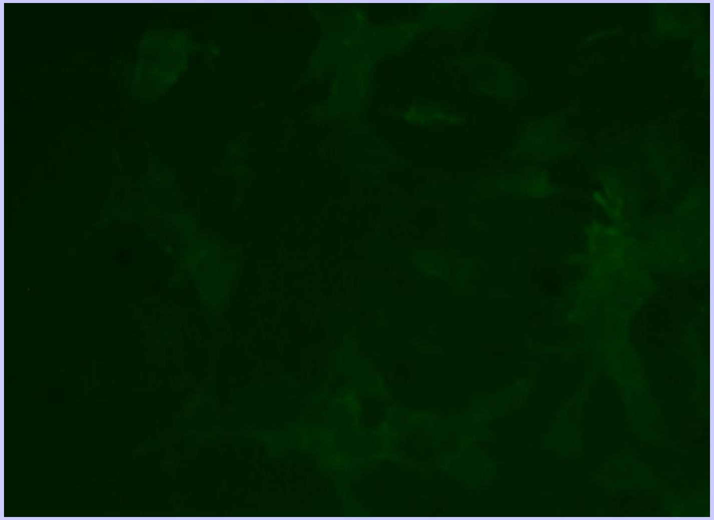

FIBROBLAST CELLS WITH SIC QDS

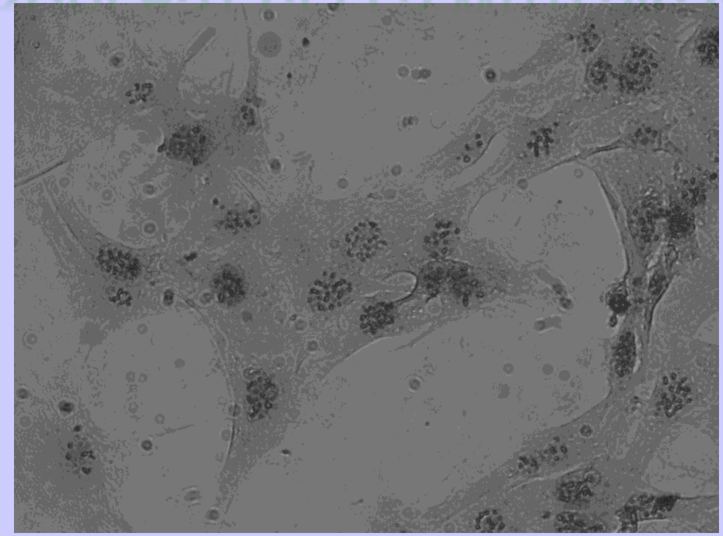

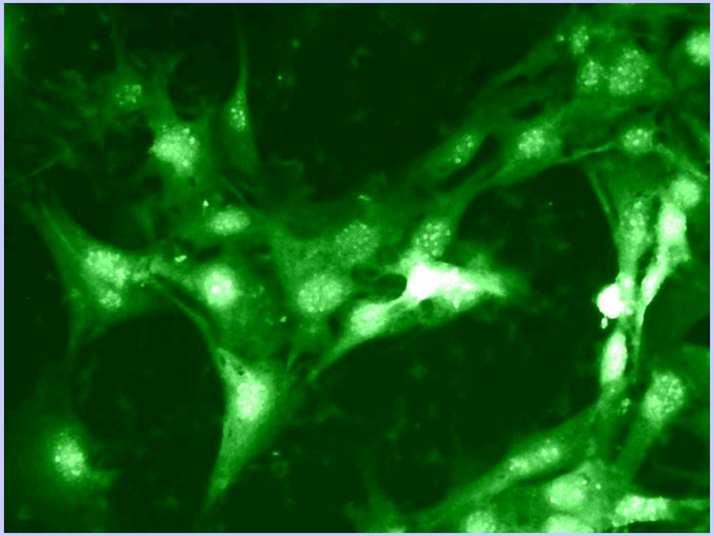

Semiconductor Nanoparticles for cell imaging

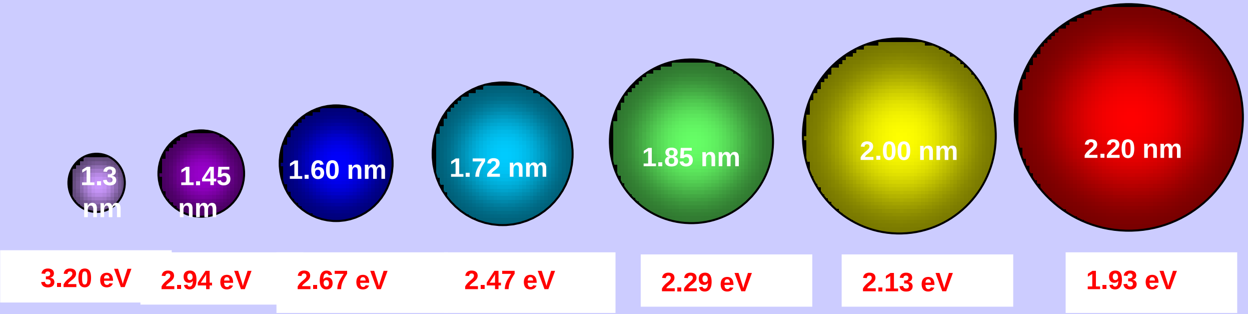

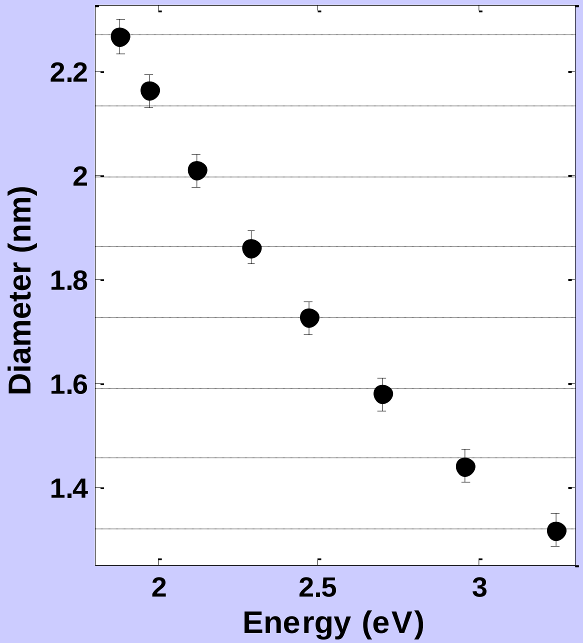

J.K. Jaiswal, S. M. Simon, *Trends in cell biology*, vol 14, 497-504 (2004)

Electroless metal introduction into the Si pores

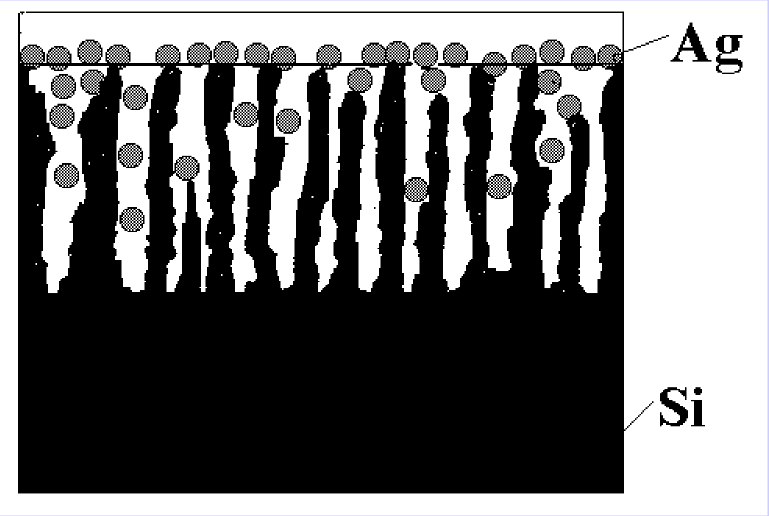

$$Ag^{+} + e_{vb}^{-} \rightarrow Ag^{0}(s)$$

$$Si(s) + 2H_2O \rightarrow SiO_2 + 4H^{+} + 4e_{vb}^{-}$$

$$SiO_2(s) + 6HF \rightarrow H_2SiF_6 + 2H_2O$$

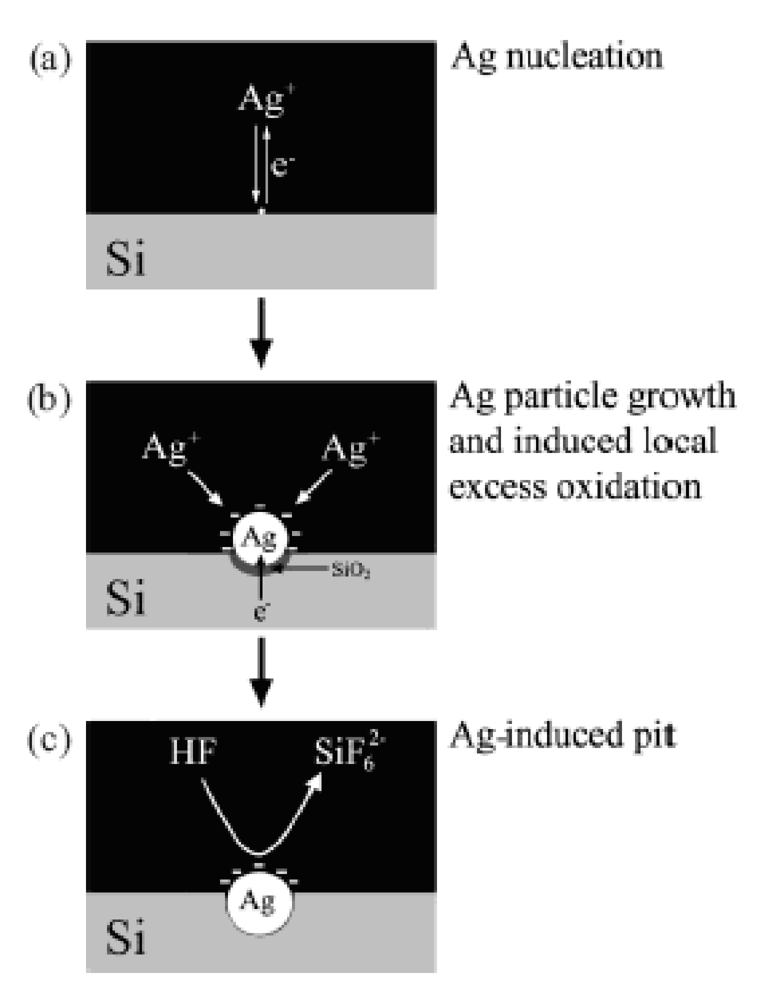

Mechanism of electroless Ag deposition on Si in HF/AgNO3 solution.

Electroless deposition of metal on Si: the working principle is the galvanic displacement reaction. The reduction of metal ions (cathodic process and oxidation of Si atoms (anodic process) occur simultaneously at Si surface, while the charge is exchanged through the Si substrate

Surface Enhanced Raman Scattering of Small Molecules from Ag coated Si pores

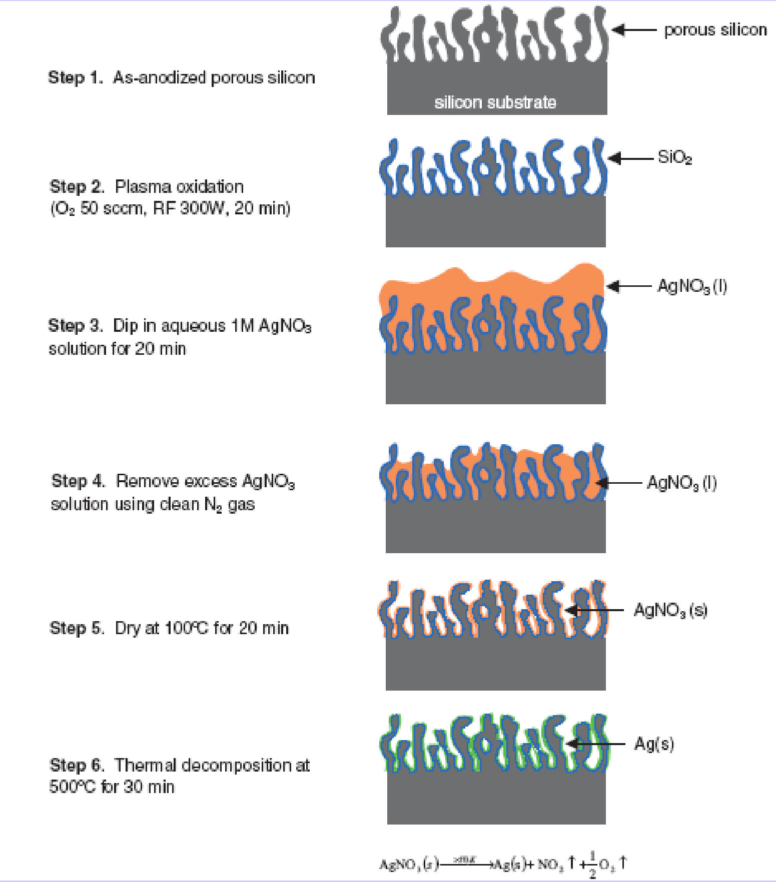

S.Chan, Adv.Mat, 2003, 15, 1595

SERS of rodamine 6G

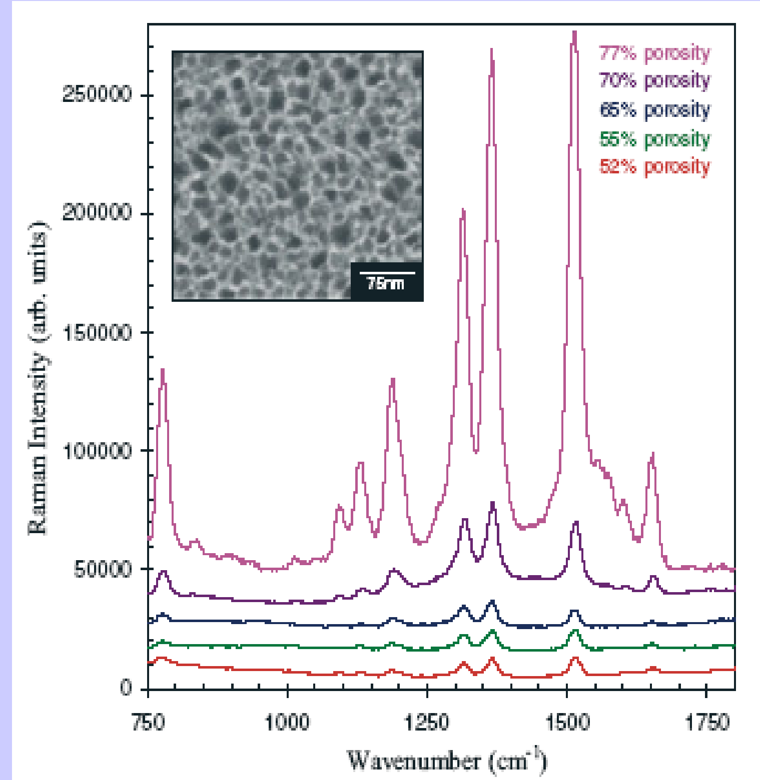

Raman spectroscopy may be used to detect nucleotides, purines or pyrimidines

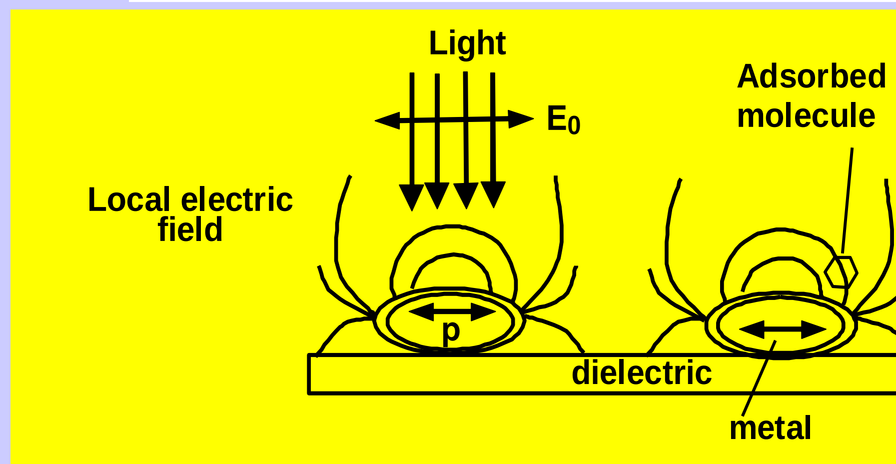

V.Tolstoy, I.Chernysheva, V.Skryshevsky, Handbook of IR spectroscopy of superthin films, Wiley, N.Y., 2003

Straining of c-Si thin film with PS substrate

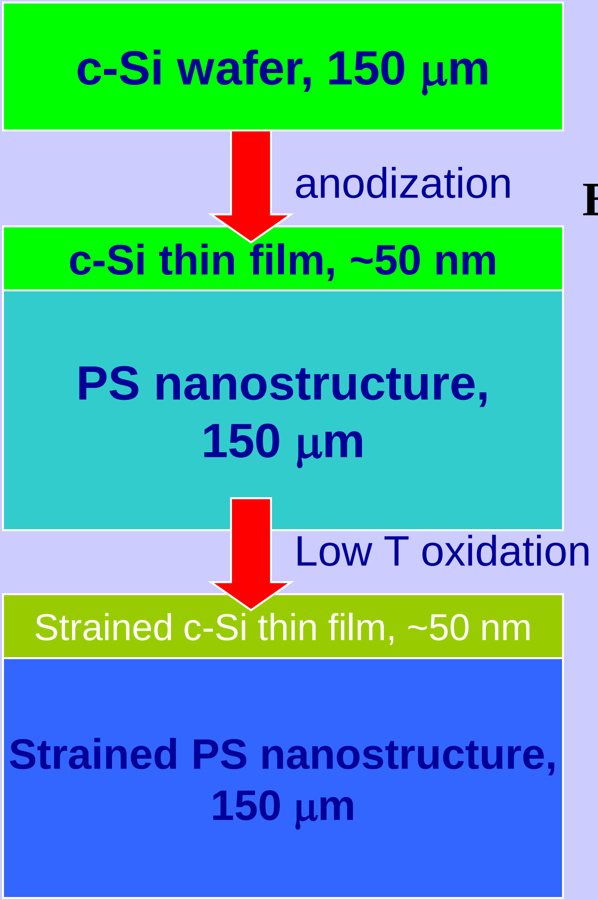

Raman spectra (LO phonon) of PS and thin c-Si films

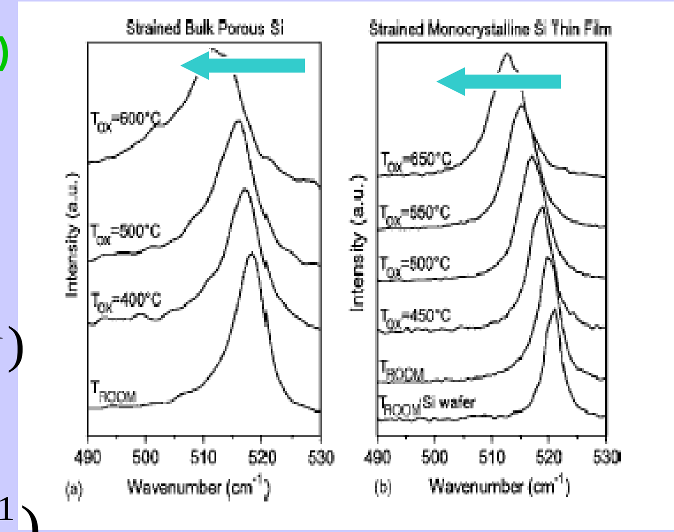

Biaxial X-Y in plane stress

$$\sigma(MPA) = -250 * \Delta\omega(cm^{-1})$$

Lattice strain

$$\xi(\%) = 0.15 * \Delta\omega(cm^{-1})$$

Up to 1.4%

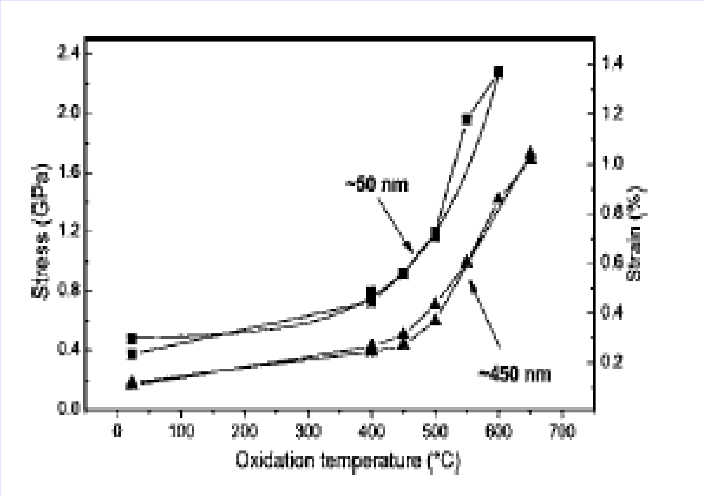

Straining of thin Si films with use of bulk partially oxidized PS nanostructure

O.Marty, T.Nychyporuk, V.Lysenko, Appl.Phys.Lett, 88, 101909, 2006